Minimal horizontal triods: Analysis and computation

Robert Nürnberg* and Paola Pozzi†

Abstract

In this article we investigate the question of finding a network configuration of minimal length connecting three given points in the Heisenberg group. After proving existence of (possibly degenerate) minimal horizontal triods, we investigate their characterization. We then formulate a horizontal curve shortening flow that deforms any given suitable initial triod into a critical point for the length functional. Numerical experiments based on a stable fully discrete finite element scheme provide useful insights into the rich landscape of this sub-Riemannian geometry.

Keywords: sub-Riemannian geometry, horizontal triods, minimal length, existence results, horizontal curve shortening flow, finite element scheme

MSC(2020): 49J05; 58J35; 65M60.

1 Introduction

In this article we investigate the classical Steiner problem in the Heisenberg group. The (first) Heisenberg group is the simplest example of a sub-Riemannian space. Thus the geometry is constrained, in the sense that motion is only allowed along a given set of directions that change from point to point.

The classical Euclidean problem of finding the path of shortest length connecting three given distinct points $P_1, P_2, P_3 \in \mathbb{R}^3$, see e.g. [16, 19, 15, 18], is now posed as the question of existence of (possibly degenerate) shortest horizontal triods of minimal length. A horizontal triod is the union of three horizontal curves connecting the points P_α, $\alpha = 1, 2, 3$, to a common junction point Σ. For a curve to be horizontal, its tangent vector must lie in a specific plane that changes from point to point. The triod is said to be degenerate if Σ coincides with one of the P_α and the corresponding curve collapses to a point. The length of the triod is given as the sum of the lengths of its component curves in an appropriate metric. Unlike the Euclidean case, where triods are unions of straight line segments, and where the Steiner problem can be treated with elementary geometry (see the beautiful presentation given in [16]), we need here some more refined mathematics.

In this work we show existence of minimal horizontal (possibly degenerate) triods and give a characterization of the minimal configurations using direct methods of calculus of variations and using some ideas from the field of minimal surfaces. We find that: if a minimal triod is composed of three curves then its projected planar curves meet at a 120 degree angle and have curvatures that sum up to zero. In particular, the projected triod is composed of lines and/or arcs of circles. If the minimal triod is degenerate, then the remaining projected curves have constant curvature but no angle condition needs to hold. Uniqueness can in general not be expected, since even a curve of minimal length connecting two given distinct points need not to be unique in the Heisenberg group (see for instance [8, § 2.3] or the direct computations provided in Remark A.2 in the Appendix).

Additionally we formulate a flow, which we call horizontal curve shortening flow, that lets a given initial horizontal triod evolve into a critical configuration for the length functional. Such evolutions are discretized by finite elements with an unconditionally stable algorithm. The simulations we propose allow for a deeper understanding of this fascinating anisotropic space. In particular, the numerical experiments show that the landscape of degenerate triods is much richer

*Dipartimento di Matematica, Università di Trento, 38123 Trento, Italy, robert.nurnberg@unitn.it

†Fakultät für Mathematik, Universität Duisburg-Essen, Thea-Leymann-Straße 9, 45127 Essen, Germany, paola.pozzi@uni-due.de

than in the Euclidean case. While in the Euclidean setting it is known that as soon as the largest angle of the triangle formed by the three points P_α, $\alpha = 1, 2, 3$, is larger or equal to 120 degrees, then the minimal configuration is given by two straight segments, see e.g. [16, 15, 18], we could not find a similar condition experimentally for the horizontal set-up (see for instance Experiments 2,3 and 4 in Section 5). Moreover, degenerate triods are clearly non-unique: Experiment 10 in Section 5 indicates the existence of a degenerate solution made up of the horizontal lift of two circles connecting three points lying on the z-axis. Any rotation around the z-axis yields another critical configuration of the same length, hence providing an infinite family of degenerate solutions.

The remainder of this article is organized as follows: in Section 2 we recall all necessary notions needed to understand the geometry of the Heisenberg group. In Section 3 we formulate the problem and provide proof of existence of minimal triods. After deriving the Euler–Lagrange equations for minimal and critical configurations, the horizontal curve shortening flow for triods is formulated. In Section 4 a finite element scheme is proposed and its stability properties are proved. Several interesting numerical simulations are given in Section 5.

Throughout this paper, we use superscripts to denote the components of a vector in $\mathbb{R}^2$ or $\mathbb{R}^3$, so that e.g. $P = (P^1, P^2, P^3)^t$ for $P \in \mathbb{R}^3$. For a vector $P \in \mathbb{R}^2$, we define the perpendicular vector by $P^\perp = \binom{P^1}{P^2}^\perp = \binom{-P^2}{P^1}$.

2 Preliminaries

We consider the Heisenberg group $\mathcal{H} = (\mathbb{R}^3, \circ)$, where $\circ$ is the group operation given by

$$\begin{pmatrix} x \\ y \\ z \end{pmatrix} \circ \begin{pmatrix} \hat{x} \\ \hat{y} \\ \hat{z} \end{pmatrix} = \begin{pmatrix} x + \hat{x} \\ y + \hat{y} \\ z + \hat{z} + \frac{1}{2}(x\hat{y} - y\hat{x}) \end{pmatrix}.$$

For comprehensive information about $\mathcal{H}$ we refer to [7], [8], and the references given there. Here we just briefly recall that $\mathcal{H}$ is a Lie group with Lie algebra generated by the left invariant vector fields

$$X_1 = \frac{\partial}{\partial x} - \frac{y}{2}\frac{\partial}{\partial z}, \qquad X_2 = \frac{\partial}{\partial y} + \frac{x}{2}\frac{\partial}{\partial z}, \qquad X_3 = \frac{\partial}{\partial z}.$$

Note that $X_3 = [X_1, X_2]$ and that $\mathcal{H}$ is a nilpotent Lie group of step 2.

With some abuse of notation we set

$$X_1(x, y, z) = \begin{pmatrix} 1 \\ 0 \\ -\frac{y}{2} \end{pmatrix}, \qquad X_2(x, y, z) = \begin{pmatrix} 0 \\ 1 \\ \frac{x}{2} \end{pmatrix}, \qquad X_3(x, y, z) = \begin{pmatrix} 0 \\ 0 \\ 1 \end{pmatrix},$$

i.e. we identify the vector fields with the associated differential operators. At each point $p = (x, y, z)^t$, the three vectors $X_i(x, y, z)$ are linear independent. We denote by $g_p(\cdot, \cdot) : \mathbb{R}^3 \times \mathbb{R}^3 \to [0, \infty)$ the inner product for which the vectors $X_i(p)$ build an orthonormal basis and set

$$|v|_g = \sqrt{g_p(v, v)} \qquad \text{for } v \in \operatorname{span}\{X_1(p), X_2(p), X_3(p)\}.$$

The horizontal tangent space at a point $p = (x, y, z)^t$ is linearly spanned by $X_1(p)$ and $X_2(p)$.

Definition 2.1. *A (sufficiently smooth) curve $\gamma : [0, 1] \to \mathcal{H}$, $\gamma = \gamma(u)$, is said to be* horizontal *if its tangent vector $\gamma'(u)$ is a linear combination of $X_1(\gamma(u))$ and $X_2(\gamma(u))$ for each $u \in [0, 1]$.*

Remark 2.1. *Note that since for $\gamma : [0, 1] \to \mathbb{R}^3$, $\gamma = \gamma(u)$ (sufficiently smooth), it holds*

$$\begin{aligned} \gamma'(u) = \gamma_u(u) &= \begin{pmatrix} \gamma_u^1(u) \\ \gamma_u^2(u) \\ \gamma_u^3(u) \end{pmatrix} \\ &= \gamma_u^1(u) X_1(\gamma(u)) + \gamma_u^2(u) X_2(\gamma(u)) + \left(\gamma_u^3(u) + \frac{1}{2}\gamma^2(u)\gamma_u^1(u) - \frac{1}{2}\gamma^1(u)\gamma_u^2(u) \right) X_3(\gamma(u)), \end{aligned}$$

we have that γ is horizontal if and only if

$$\gamma_u^3 = -\frac{1}{2}\gamma^2\gamma_u^1 + \frac{1}{2}\gamma^1\gamma_u^2 \quad \text{in } [0,1]. \tag{2.1}$$

In particular, for a horizontal curve its third space dimension component γ^3 is determined by the other two space components via

$$\gamma^3(u) = \gamma^3(0) + \int_0^u \left(-\frac{1}{2}\gamma^2(\xi)\gamma_u^1(\xi) + \frac{1}{2}\gamma^1(\xi)\gamma_u^2(\xi)\right) d\xi, \tag{2.2}$$

or, equivalently,

$$\gamma^3(u) = \gamma^3(1) - \int_u^1 \left(-\frac{1}{2}\gamma^2(\xi)\gamma_u^1(\xi) + \frac{1}{2}\gamma^1(\xi)\gamma_u^2(\xi)\right) d\xi. \tag{2.3}$$

Finally, note that for a horizontal curve γ we have

$$|\gamma_u(u)|_g = \sqrt{(\gamma_u^1(u))^2 + (\gamma_u^2(u))^2},$$

and its length is given by

$$L(\gamma) = \int_0^1 |\gamma_u(u)|_g du = \int_0^1 \sqrt{(\gamma_u^1(u))^2 + (\gamma_u^2(u))^2} du.$$

The length functional is a geometric functional in the sense that it is invariant under reparametrizations of the curve γ. The same holds for the functional (cf. with (2.2)*)*

$$\mathfrak{G}(\gamma) := \int_0^1 \left(-\frac{1}{2}\gamma^2(u)\gamma_u^1(u) + \frac{1}{2}\gamma^1(u)\gamma_u^2(u)\right) du \tag{2.4}$$

when restricting to reparametrizations that keep the same orientation of the curve.

Definition 2.2 (Projected curve and horizontal lift)**.** *Given a horizontal curve $\gamma : [0,1] \to \mathcal{H}$, we denote by $c : [0,1] \to \mathbb{R}^2$, $c = (\gamma^1, \gamma^2)^t$, the projected curve of γ in the plane $\{z = 0\}$.*

Vice-versa, given a planar curve $c : [0,1] \to \mathbb{R}^2$ we call horizontal lift *of c any map $\gamma : [0,1] \to \mathcal{H}$, $\gamma = (\gamma^1, \gamma^2, \gamma^3)^t$, with $(\gamma^1, \gamma^2)^t = c$ and γ^3 satisfying* (2.2)*.*

Remark 2.2. *Clearly, the lift of c is only unique up to specifying $\gamma^3(0)$, for example. Hence we say that γ is the horizontal lift of c starting at $P \in \mathbb{R}^3$ if in addition $\gamma(0) = P$, recall* (2.2)*. Similarly, we say that γ is the horizontal lift of c ending at $Q \in \mathbb{R}^3$ if $\gamma(1) = Q$, recall* (2.3)*.*

Remark 2.3 (Geometrical interpretation for the z-component of a horizontal curve)**.** *Note that for a horizontal curve joining the points $P = \gamma(0)$ and $Q = \gamma(1) \in \mathbb{R}^3$, equation* (2.2) *yields that*

$$|Q^3 - P^3| = \left|\int_0^1 \frac{1}{2}\begin{pmatrix}\gamma^1(u)\\ \gamma^2(u)\end{pmatrix} \cdot \begin{pmatrix}-\gamma_u^2(u)\\ \gamma_u^1(u)\end{pmatrix} du\right| = \left|\int_0^1 \frac{1}{2} c(u) \cdot c_u^\perp(u) du\right| = |\textit{oriented area}(S)|,$$

where S is the portion in the plane swept by the vector $c(u)$ of the projected curve c.

For example, a planar semicircle of radius $R > 0$, connecting, say, the points $P = 0$ and $Q = (2R, 0, 0)^t$, is not *a horizontal curve, since $|Q^3 - P^3| = 0$, while the swept region has area $\frac{\pi}{2}R^2$. On the other hand, any planar straight line segment that goes through the origin is horizontal.*

Lemma 2.4. *For $a = (a^1, a^2, a^3)^t \in \mathbb{R}^3$ let $\tau_a(x, y, z) := (a^1, a^2, a^3)^t \circ (x, y, z)^t$ denote the left translation. If $\gamma : [0,1] \to \mathcal{H}$ is horizontal, then so is the curve $u \mapsto \tau_a(\gamma(u))$. Moreover, $L(\gamma) = L(\tau_a(\gamma))$.*

Proof. The claims follow by direct computation. □

Remark 2.5. *Left translation of a horizontal curve $\gamma : [0,1] \to \mathcal{H}$ by $a = (-\gamma^1(0), -\gamma^2(0), -\gamma^3(0))^t$ ensures that the translated curve $\tau_a(\gamma)$ starts at the origin.*

Remark 2.6. *For $a = (0, 0, a^3)^t$ we have that $\tau_a(\gamma(u)) = \gamma(u) + (0, 0, a^3)^t$.*

We recall the following important connectivity theorem.

Proposition 2.7. *Any two points in $\mathcal{H}$ can be connected by a horizontal smooth curve.*

Proof. See, for instance, [7, §1.3]. □

2.1 On tangent, normal, and curvature vectors

Definition 2.3. *We say that a (sufficiently smooth) horizontal curve $\gamma : [0,1] \to \mathcal{H}$ is regular if $|\gamma_u(u)|_g \neq 0$ for all $u \in [0,1]$.*

To motivate the definition of curvature vector for horizontal curves, let us first recall the following lemma:

Lemma 2.8. *For a sufficiently smooth regular horizontal curve $\gamma : [0,1] \to \mathbb{R}^3$ let*

$$\vec{k}(u) := \frac{1}{|\gamma_u(u)|_g}\left(\frac{1}{|\gamma_u(u)|_g}\begin{pmatrix}\gamma_u^1(u)\\ \gamma_u^2(u)\end{pmatrix}\right)_u \quad \in \mathbb{R}^2.$$

With

$$k(u) := \frac{\gamma_{uu}^2(u)\gamma_u^1(u) - \gamma_u^2(u)\gamma_{uu}^1(u)}{((\gamma_u^1(u))^2 + (\gamma_u^2(u))^2)^{\frac{3}{2}}} \tag{2.5}$$

there holds

$$\vec{k}(u) = k(u)\frac{1}{|\gamma_u(u)|_g}\begin{pmatrix}-\gamma_u^2(u)\\ \gamma_u^1(u)\end{pmatrix}.$$

Proof. The claim follows by direct computation. □

Note that $\vec{k}$ is the standard Euclidean curvature vector of the projected planar curve $c : I \to \mathbb{R}^2$, $c(u) := (\gamma^1(u), \gamma^2(u))^t$, whose arc length is given by $ds = \sqrt{(\gamma_u^1(u))^2 + (\gamma_u^2(u))^2}du$. Thus $\vec{k} = \partial_{ss}c$.

In analogy to the Euclidean case we provide the following definition of *horizontal curvature vector.*

Lemma 2.9. *For a sufficiently smooth regular horizontal curve $\gamma : [0,1] \to \mathbb{R}^3$ we define the horizontal unit tangent*

$$\begin{aligned} T(u) &:= \frac{1}{|\gamma_u(u)|_g}\begin{pmatrix}\gamma_u^1(u)\\ \gamma_u^2(u)\\ \gamma_u^3(u)\end{pmatrix} = \frac{1}{|\gamma_u(u)|_g}\begin{pmatrix}\gamma_u^1(u)\\ \gamma_u^2(u)\\ -\frac{1}{2}\gamma^2(u)\gamma_u^1(u) + \frac{1}{2}\gamma^1(u)\gamma_u^2(u)\end{pmatrix} \\ &= \frac{\gamma_u^1(u)}{|\gamma_u(u)|_g}X_1(\gamma(u)) + \frac{\gamma_u^2(u)}{|\gamma_u(u)|_g}X_2(\gamma(u)), \end{aligned} \tag{2.6}$$

the horizontal normal vector

$$N(u) := -\frac{\gamma_u^2(u)}{|\gamma_u(u)|_g}X_1(\gamma(u)) + \frac{\gamma_u^1(u)}{|\gamma_u(u)|_g}X_2(\gamma(u)) = \frac{1}{|\gamma_u(u)|_g}\begin{pmatrix}-\gamma_u^2(u)\\ \gamma_u^1(u)\\ \frac{1}{2}\gamma^2(u)\gamma_u^2(u) + \frac{1}{2}\gamma^1(u)\gamma_u^1(u)\end{pmatrix}, \tag{2.7}$$

and the horizontal curvature vector

$$\vec{k}_g(u) := \frac{1}{|\gamma_u(u)|_g}T_u(u).$$

Then we have that

$$\begin{aligned} \vec{k}_g(u) &= k(u)N(u) \\ &= \begin{pmatrix}\vec{k}(u)\\ \frac{k(u)}{|\gamma_u(u)|_g}(\frac{1}{2}\gamma^2(u)\gamma_u^2(u) + \frac{1}{2}\gamma^1(u)\gamma_u^1(u))\end{pmatrix} = \frac{k(u)}{|\gamma_u(u)|_g}\begin{pmatrix}-\gamma_u^2(u)\\ \gamma_u^1(u)\\ \frac{1}{2}\gamma^2(u)\gamma_u^2(u) + \frac{1}{2}\gamma^1(u)\gamma_u^1(u)\end{pmatrix}, \end{aligned} \tag{2.8}$$

where $\vec{k}$ and k are as in Lemma 2.8.

Proof. It follows from Lemma 2.8 that we only need to verify the third component in (2.8). On recalling (2.1), we have that

$$\gamma_u^3 = \frac{1}{2}(\gamma^1\gamma_u^2 - \gamma^2\gamma_u^1), \qquad \gamma_{uu}^3 = \frac{1}{2}(\gamma^1\gamma_{uu}^2 - \gamma^2\gamma_{uu}^1). \tag{2.9}$$

Hence we can compute

$$\begin{aligned}\frac{1}{|\gamma_u(u)|_g}T_u^3(u) &= \frac{1}{|\gamma_u|_g}\left(\frac{\gamma_u^3}{|\gamma_u|_g}\right)_u = \frac{1}{|\gamma_u|_g}\left(\frac{\gamma_{uu}^3}{|\gamma_u|_g} - \frac{\gamma_u^3}{|\gamma_u|_g^3}(\gamma_u^2\gamma_{uu}^2 + \gamma_u^1\gamma_{uu}^1)\right)\\ &= \frac{1}{|\gamma_u|_g}\frac{1}{|\gamma_u|_g^3}\left(\gamma_{uu}^3((\gamma_u^1)^2 + (\gamma_u^2))^2 - \gamma_u^3(\gamma_u^2\gamma_{uu}^2 + \gamma_u^1\gamma_{uu}^1)\right)\\ &= \frac{1}{|\gamma_u|_g}\frac{k(u)}{2}(\gamma^2\gamma_u^2 + \gamma^1\gamma_u^1),\end{aligned}$$

where we have used (2.9) and (2.5) in the last equality. □

Note that

$$g(T,T) = 1, \quad g(N,N) = 1, \quad g(T,N) = 0, \quad g(T,X_3) = 0, \quad g(N,X_3) = 0, \tag{2.10}$$

so that $\{T, N, X_3\}$ provides another orthonormal frame with respect to the inner product $g(\cdot,\cdot)$.

Finally, let us recall how time dependent motion of a curve in its N direction can be corrected so that the curve $\gamma(t)$ stays horizontal along the flow (see [11, Lemma 2]):

Lemma 2.10. *Let $\gamma_0 : [0,1] \to \mathbb{R}^3$ be a horizontal regular curve. Suppose that the (sufficiently smooth) family of curves $\gamma : [0,\hat{T}) \times [0,1] \to \mathbb{R}^3$, $\gamma = \gamma(t,u)$, satisfies $\gamma(0,\cdot) = \gamma_0(\cdot)$ and*

$$\gamma_t(t,u) = m(t,u)N(t,u) - \left(\int_0^u m(t,\xi)|\gamma_u(t,\xi)|_g d\xi\right) X_3(\gamma(t,u))$$

for some sufficiently smooth $m : [0,\hat{T}) \times [0,1] \to \mathbb{R}$, with $N(t,\cdot)$ as in (2.7), and $|\gamma_u(t,u)|_g = \sqrt{(\gamma_u^1(t,u))^2 + (\gamma_u^2(t,u))^2} \neq 0$ for all $(t,u) \in [0,\hat{T}) \times [0,1]$. Then $\gamma(t)$ is horizontal for any $t \in [0,\hat{T})$. [1]

Proof. We compute

$$\begin{aligned}\left(\gamma_u^3 + \frac{1}{2}\gamma^2\gamma_u^1 - \frac{1}{2}\gamma^1\gamma_u^2\right)_t &= (\gamma_t^3)_u - \frac{1}{2}\gamma_t^1\gamma_u^2 - \frac{1}{2}\gamma^1(\gamma_t^2)_u + \frac{1}{2}\gamma_t^2\gamma_u^1 + \frac{1}{2}\gamma^2(\gamma_t^1)_u\\ &= \left(\frac{m}{|\gamma_u|_g}\frac{1}{2}(\gamma^2\gamma_u^2 + \gamma^1\gamma_u^1)\right)_u - m|\gamma_u|_g - \frac{1}{2}\gamma_u^2\Big(-m\frac{\gamma_u^2}{|\gamma_u|_g}\Big) - \frac{1}{2}\gamma^1\Big(m\frac{\gamma_u^1}{|\gamma_u|_g}\Big)_u\\ &\quad + \frac{1}{2}\gamma_u^1\Big(m\frac{\gamma_u^1}{|\gamma_u|_g}\Big) + \frac{1}{2}\gamma^2\Big(-m\frac{\gamma_u^2}{|\gamma_u|_g}\Big)_u = 0.\end{aligned}$$

The claim then follows from the smoothness assumptions, the initial curve being horizontal and (2.1). □

We remark that motion in the T direction maintains the horizontal property:

Lemma 2.11. *Let $\gamma_0 : [0,1] \to \mathbb{R}^3$ be a horizontal regular curve. Suppose that the (sufficiently smooth) family of curves $\gamma : [0,\hat{T}) \times [0,1] \to \mathbb{R}^3$, $\gamma = \gamma(t,u)$, satisfies $\gamma(0,\cdot) = \gamma_0(\cdot)$ and*

$$\gamma_t(t,u) = q(t,u)T(t,u)$$

for some sufficiently smooth $q : [0,\hat{T}) \times [0,1] \to \mathbb{R}$, with $T(t,\cdot)$ as in (2.6), and $|\gamma_u(t,u)|_g = \sqrt{(\gamma_u^1(t,u))^2 + (\gamma_u^2(t,u))^2} \neq 0$ for all $(t,u) \in [0,\hat{T}) \times [0,1]$. Then $\gamma(t)$ is horizontal for any $t \in [0,\hat{T})$.

Proof. As in the previous lemma we compute

$$\begin{aligned}\left(\gamma_u^3 + \frac{1}{2}\gamma^2\gamma_u^1 - \frac{1}{2}\gamma^1\gamma_u^2\right)_t &= (\gamma_t^3)_u - \frac{1}{2}\gamma_t^1\gamma_u^2 - \frac{1}{2}\gamma^1(\gamma_t^2)_u + \frac{1}{2}\gamma_t^2\gamma_u^1 + \frac{1}{2}\gamma^2(\gamma_t^1)_u\\ &= \left(\frac{q}{|\gamma_u|_g}(-\frac{1}{2}\gamma^2\gamma_u^1 + \frac{1}{2}\gamma^1\gamma_u^2)\right)_u - \frac{1}{2}\gamma_u^2 q\frac{\gamma_u^1}{|\gamma_u|_g} - \frac{1}{2}\gamma^1\left(q\frac{\gamma_u^2}{|\gamma_u|_g}\right)_u\\ &\quad + \frac{1}{2}\gamma_u^2 q\frac{\gamma_u^1}{|\gamma_u|_g} + \frac{1}{2}\gamma^2\left(q\frac{\gamma_u^1}{|\gamma_u|_g}\right)_u = \frac{1}{2}\gamma_u^1\gamma_u^2\frac{q}{|\gamma_u|_g} - \frac{1}{2}\gamma_u^2\gamma_u^1\frac{q}{|\gamma_u|_g} = 0.\end{aligned}$$

The claim then follows as before from the smoothness assumptions and the initial curve being horizontal. □

[1] The same result applies with $\gamma_t(t,u) = m(t,u)N(\gamma(t,u)) + \left(\int_u^1 m(t,\xi)|\gamma_u(t,\xi)|_g d\xi\right) X_3(\gamma(t,u))$.

2.2 Horizontal curves of minimal length

The existence of a length minimizing curve connecting any two given points in $\mathcal{H}$ is a well studied topic. It is discussed for instance in [23, §1.6 and Appendix D.4], [7], and [8, §2.3], but can also be derived anew with the techniques described below in Section 3.

In the following we derive the Euler–Lagrange equations for curves minimizing the length functional and investigate their solutions, since these computations will be useful later on in Section 3.

Remark 2.12 (Euler–Lagrange equations for length minimizing curves)**.** *Following the ideas presented in Remark 2.1, to find a shortest horizontal curve $\gamma : [0,1] \to \mathbb{R}^3$ connecting two given distinct points $P = (P^1, P^2, P^3)^t$ and $Q = (Q^1, Q^2, Q^3)^t \in \mathbb{R}^3$, it is natural to consider the class of projected curves*

$$\mathcal{C}_{single} := \{c \in C^1([0,1], \mathbb{R}^2) \,:\, c(0) = (P^1, P^2)^t,\ c(1) = (Q^1, Q^2)^t\}$$

with Euclidean length

$$L_E(c) := \int_0^1 |c_u(u)| du,$$

where $|\cdot|$ denotes the Euclidean norm, and solve the problem

$$\min\{L_E(c) \,:\, c \in \mathcal{C}_{single} \text{ and } G(c) = Q^3 - P^3\}, \tag{2.11}$$

where, similarly to (2.4)*,*

$$G(c) = \int_0^1 \left(-\frac{1}{2} c^2(u) c_u^1(u) + \frac{1}{2} c^1(u) c_u^2(u) \right) du. \tag{2.12}$$

The horizontal lift, starting at P, of a minimizer for (2.11)*, is then a horizontal length minimizing curve connecting P and Q.*

Note that for $\varphi \in C^\infty([0,1], \mathbb{R}^2)$ the first variation of G at c in the direction φ is given by

$$\begin{aligned}
\delta G(c)(\varphi) = \frac{d}{d\epsilon}\Big|_{\epsilon=0} G(c + \epsilon\varphi) &= \frac{1}{2} \int_0^1 \varphi^1 c_u^2 + c^1 \varphi_u^2 - c^2 \varphi_u^1 - \varphi^2 c_u^1 du \\
&= \frac{1}{2} [c^1 \varphi^2 - c^2 \varphi^1]_0^1 + \int_0^1 \varphi^1 c_u^2 - \varphi^2 c_u^1 du \\
&= \frac{1}{2} [c^1 \varphi^2 - c^2 \varphi^1]_0^1 + \int_0^1 \begin{pmatrix} \varphi^1 \\ \varphi^2 \end{pmatrix} \cdot \begin{pmatrix} c_u^2 \\ -c_u^1 \end{pmatrix} du.
\end{aligned} \tag{2.13}$$

In particular, we have that if $c \in \mathcal{C}_{single}$ is a regular curve (i.e. $|c'| \neq 0$ in $[0,1]$) then $\delta G(c)(\varphi)$ does not vanish for all $\varphi \in C_0^\infty((0,1), \mathbb{R}^2)$. It then follows from [6, Proposition 1.17, Proposition 1.2] that a regular weak minimizer for problem (2.11) *is such that there exists $\lambda \in \mathbb{R}$ such that*

$$\delta L_E(c)(\varphi) + \lambda \delta G(c)(\varphi) = 0 \qquad \forall\, \varphi \in C_0^\infty((0,1), \mathbb{R}^2).$$

Moreover, if $c \in C^2([0,1], \mathbb{R}^2)$, then

$$\begin{aligned}
0 &= -\int_0^1 \frac{1}{|c'|} \left(\frac{1}{|c'|} \begin{pmatrix} c_u^1 \\ c_u^2 \end{pmatrix} \right)_u \cdot \begin{pmatrix} \varphi^1 \\ \varphi^2 \end{pmatrix} |c'| du + \lambda \int_0^1 \begin{pmatrix} \varphi^1 \\ \varphi^2 \end{pmatrix} \cdot \frac{1}{|c'|} \begin{pmatrix} c_u^2 \\ -c_u^1 \end{pmatrix} |c'| du \\
&= -\int_0^1 \vec{k} \cdot \begin{pmatrix} \varphi^1 \\ \varphi^2 \end{pmatrix} |c'| du - \lambda \int_0^1 \begin{pmatrix} \varphi^1 \\ \varphi^2 \end{pmatrix} \cdot \frac{1}{|c'|} \begin{pmatrix} -c_u^2 \\ c_u^1 \end{pmatrix} |c'| du.
\end{aligned}$$

for all test functions $\varphi \in C_0^\infty((0,1), \mathbb{R}^2)$. It follows that λ can be expressed through the following equation

$$\int_0^1 k(u) |c_u(u)| du + \lambda L_E(c) = 0.$$

Summing up, a horizontal length minimizing curve $\gamma : [0,1] \to \mathcal{H}$ connecting two given distinct points P and Q in $\mathbb{R}^3$ is a horizontal curve such that (in the notation of Lemma 2.8)

$$k(u) + \lambda = 0 \text{ in } (0,1), \qquad \text{with} \qquad \lambda = -\frac{\int_0^1 k(u) |\gamma_u(u)|_g du}{L(\gamma)}. \tag{2.14}$$

From (2.14) we observe that length minimizing curves in $\mathcal{H}$ can be straight segments or smooth curves whose projection onto the plane are arcs of circles. In Remark A.2, in the appendix, we derive an explicit solution formula and recognize the surprising fact that there is a unique length minimizing curve connecting the origin to a point $Q = (Q^1, Q^2, Q^3)^t \neq 0$ if $(Q^1, Q^2)^t \neq 0$, whereas we have infinitely many length minimizing curves connecting the origin to $Q = (0, 0, Q^3)^t$.

3 Horizontal triods

In the following we consider triods of horizontal curves. Given are three distinct points $P_\alpha = (P^1_\alpha, P^2_\alpha, P^3_\alpha)^t \in \mathbb{R}^3$, $\alpha = 1, 2, 3$. We consider three regular horizontal curves $\gamma_\alpha : [0, 1] \to \mathbb{R}^3$, $\gamma_\alpha = \gamma_\alpha(u)$, connecting the points P_α to a common junction point, which we denote by Σ, i.e.

$$\begin{aligned} &\gamma_\alpha(1) = P_\alpha, \qquad \alpha = 1, 2, 3, \\ &\gamma_1(0) = \gamma_2(0) = \gamma_3(0) =: \Sigma \in \mathbb{R}^3, \end{aligned}$$

with associated functional

$$L(\Gamma) = \sum_{\alpha=1}^{3} L(\gamma_\alpha) \tag{3.1}$$

for $\Gamma = (\gamma_1, \gamma_2, \gamma_3)$ the horizontal triod. In the following we say that a horizontal triod Γ is regular if all its curves γ_α are regular (according to Definition 2.3). Our goal is to study minimal configurations for L. First of all, we show existence in a proper class of functions.

3.1 Existence of a minimal configuration

As in the case of a single curve, we can reduce the problem to a constrained planar one. We denote by

$$\mathcal{C} := \{\Gamma_c = (c_1, c_2, c_3) \,:\, c_\alpha \in H^{1,1}((0, 1), \mathbb{R}^2), c_\alpha(1) = (P^1_\alpha, P^2_\alpha)^t, \alpha = 1, 2, 3,\ c_1(0) = c_2(0) = c_3(0)\}$$

the class of natural admissible functions with associated functional

$$L_E(\Gamma_c) := \sum_{\alpha=1}^{3} L_E(c_\alpha).$$

Note that because of the embedding of $H^{1,1}$ into the class of continuous maps, the pointwise boundary conditions are meaningful. In the following we set $\overline{\Sigma} := c_1(0) = c_2(0) = c_3(0)$ to be the planar junction point. We want to solve the problem

$$\min\{L_E(\Gamma_c) \,:\, \Gamma_c \in \mathcal{C}, \quad G(c_1) - P^3_1 = G(c_2) - P^3_2 = G(c_3) - P^3_1\},$$

where G is as in (2.12) (recall also (2.4) and (2.2)). The horizontal lift of a minimal planar triod Γ_c, where each curve c_α is lifted to a horizontal curve γ_α ending at P_α, is then a horizontal minimal triod.

Observe that the projected points $\overline{P}_\alpha := (P^1_\alpha, P^2_\alpha)^t$, $\alpha = 1, 2, 3$, need not be distinct, despite the fact that the original points P_α are. However, whenever two projected points coincide, say $\overline{P}_\alpha = (P^1_\alpha, P^2_\alpha)^t = (P^1_\beta, P^2_\beta)^t = \overline{P}_\beta$ for some $\alpha, \beta \in \{1, 2, 3\}$, then their third space component must be different, i.e. $P^3_\alpha \neq P^3_\beta$ if $\alpha \neq \beta$. On the other hand, if $P^3_\alpha = P^3_\beta$ for $\alpha \neq \beta$, then $\overline{P}_\alpha \neq \overline{P}_\beta$. This implies that for any triod $\Gamma_c \in \mathcal{C}$ satisfying the constraint $G(c_1) - P^3_1 = G(c_2) - P^3_2 = G(c_3) - P^3_1$, at most one curve c_α can reduce to a constant map mapping to a point (in which case $G(c_\alpha) = 0$). The horizontal lift Γ of such a configuration corresponds to a horizontal triod in which the junction point Σ has "collapsed" to one of the points P_α and one curve of Γ has reduced to a point: we refer to such a horizontal triod as a degenerate one.

Following the ideas presented in [6, §5.9] we give the following definition.

Definition 3.1. *We say that a curve $c \in H^{1,1}((0, 1), \mathbb{R}^2)$, $c = c(u)$, is* quasinormal *if $|c_u| = L_E(c) > 0$ in $(0, 1)$. A triod $\Gamma_c \in \mathcal{C}$ is quasinormal if all its components c_α, $\alpha = 1, 2, 3$, are quasinormal. Note that the planar junction point $\overline{\Sigma}$ of a quasinormal triod might coincide with one of the projected points $\overline{P}_\alpha$.*

We say that a triod $\Gamma_c \in \mathcal{C}$ is degenerate *if exactly one of its components is a constant map. In other words, if the junction point $\overline{\Sigma}$ coincides with one of the $\overline{P}_\alpha$ and the corresponding curve (starting and ending in the junction point) degenerates to one point. A degenerate triod is said to be quasinormal if its two remaining curves are quasinormal.*

Instead of working with the length functional, it is advantageous to exploit the properties of the Dirichlet functional, which is well known to "dominate" the length functional in a convenient way (see [6, §5.9] and [17] from which we have borrowed several ideas). Thus we study the following problem. Let

$$\mathcal{C}_D := \{\Gamma_c = (c_1, c_2, c_3) \in \mathcal{C} \,:\, c_\alpha \in H^{1,2}((0,1), \mathbb{R}^2)\}$$

and

$$D(\Gamma_c) := \frac{1}{2}\sum_{\alpha=1}^{3}\int_0^1 |(c_\alpha)_u|^2 du \geq 0.$$

For $1 \geq \epsilon > 0$ let us consider the ϵ-problem:

$$\min\{(L_E(\Gamma_c))^2 + \epsilon D(\Gamma_c) \,:\, \Gamma_c \in \mathcal{C}_D, \quad G(c_1) - P_1^3 = G(c_2) - P_2^3 = G(c_3) - P_1^3\}. \tag{3.2}$$

To prove existence of a minimizer, we apply standard direct methods of calculus of variations. More precisely, let $\Gamma_{c_n} \in \mathcal{C}_D$, $n \in \mathbb{N}$, be a minimizing sequence satisfying the integral constraints given in (3.2). Without loss of generality, we may assume that

$$(L_E(\Gamma_{c_n}))^2 + \epsilon D(\Gamma_{c_n}) \leq (L_E(\Gamma_{c_1}))^2 + \epsilon D(\Gamma_{c_1}) \leq (L_E(\Gamma_{c_1}))^2 + D(\Gamma_{c_1}) =: C_0 \qquad \forall n \in \mathbb{N}.$$

It follows that

$$\|\partial_u(c_{n,\alpha})\|_{L^2(0,1)} \leq C(\epsilon) \qquad \text{for all } n \in \mathbb{N}, \alpha = 1,2,3,$$

and, using the fact that the fundamental theorem of calculus holds for maps in $H^{1,m}(0,1)$, $m \geq 1$, and

$$\begin{aligned} |c_{n,\alpha}(u)| &\leq |c_{n,\alpha}(u) - c_{n,\alpha}(1)| + |P_\alpha| \leq |P_\alpha| + \int_0^1 |\partial_u(c_{n,\alpha})(u)| du \\ &\leq |P_\alpha| + \|\partial_u(c_{n,\alpha})\|_{L^2(0,1)} \leq C(\epsilon) \text{ for all } u \in [0,1], \end{aligned} \tag{3.3}$$

we obtain

$$\|c_{n,\alpha}\|_{C([0,1])} \leq C(\epsilon) \text{ for any } n \in \mathbb{N}, \quad \alpha = 1,2,3,$$

so that

$$\|c_{n,\alpha}\|_{H^{1,2}(0,1)} \leq C(\epsilon) \text{ for any } n \in \mathbb{N}, \quad \alpha = 1,2,3,$$

yielding the existence of a subsequence converging weakly in $H^{1,2}(0,1)$. Moreover, for any $u_1, u_2 \in [0,1]$ we have that

$$|c_{n,\alpha}(u_1) - c_{n,\alpha}(u_2)| \leq \|\partial_u(c_{n,\alpha})\|_{L^2(0,1)}|u_1 - u_2|^{\frac{1}{2}} \leq C(\epsilon)|u_1 - u_2|^{\frac{1}{2}} \text{ for all } n \in \mathbb{N}, \quad \alpha = 1,2,3,$$

so that using the Theorem of Ascoli–Arzelà we infer the existence of $\Gamma_{c_\epsilon} \in \mathcal{C}_D \cap C^{0,\frac{1}{2}}([0,1])$ to which a subsequence of Γ_{c_n} converges uniformly on $[0,1]$, as well as weakly in $H^{1,2}(0,1)$ (where the convergence is meant componentwise). It is easy to verify that the triod Γ_{c_ϵ} satisfies also the constraints given in (3.2).

Using that the Dirichlet functional is sequentially lower semicontinuous with respect to weak convergence in $H^{1,2}$, and that the length functional L_E is sequentially lower semicontinuous with respect to weak convergence in $H^{1,m}$ for any $m \geq 1$ (cf. for instance [9, Theorem 1.3] or [6, Theorem 3.5, Remark 2]), we infer that Γ_{c_ϵ} is a minimum for the problem formulated in (3.2), satisfying

$$(L_E(\Gamma_{c_\epsilon}))^2 + \epsilon D(\Gamma_{c_\epsilon}) \leq C_0.$$

Next, since the functionals L_E and G are invariant under smooth reparametrizations that keep the orientation of the curve c, we infer by taking inner variations (see for instance [6, Proposition 1.14, Remark 3]) for any single component map of the triod Γ_{c_ϵ} that $|(c_{\epsilon,\alpha})_u| = \textit{constant}$ for any $\alpha = 1,2,3$, yielding that we have even more regularity, namely

$$\Gamma_{c_\epsilon} \in \mathcal{C}_D \cap C^{0,1}([0,1]).$$

It could happen that the junction point of the minimal triod Γ_{c_ϵ} coincides with one of the points $\overline{P}_\alpha$, and its corresponding component could also reduce to a point. In other words, it might be convenient in the minimization procedure for one curve to disappear entirely by mapping the interval $[0,1]$ to a single point. In any case, the minimal configuration (may it be degenerate or not) is a quasinormal configuration according to Definition 3.1.

Summarizing our findings so far we can say that (for an arbitrary $0 < \epsilon \leq 1$)

$$\begin{aligned}
&(L_E(\Gamma_{c_\epsilon}))^2 + \epsilon D(\Gamma_{c_\epsilon}) \\
&\quad = \inf\{(L_E(\Gamma_{\tilde{c}}))^2 + \epsilon D(\Gamma_{\tilde{c}}) \,:\, \Gamma_{\tilde{c}} \in \mathcal{C}_D, \quad G(\tilde{c}_1) - P_1^3 = G(\tilde{c}_2) - P_2^3 = G(\tilde{c}_3) - P_1^3\} \\
&\quad \leq \inf\{(L_E(\Gamma_{\tilde{c}}))^2 + \epsilon D(\Gamma_{\tilde{c}}) \,:\, \Gamma_{\tilde{c}} \in \mathcal{C}_D \cap C^{0,1}, \Gamma_{\tilde{c}} \text{ quasinormal}, \\
&\qquad\qquad G(\tilde{c}_1) - P_1^3 = G(\tilde{c}_2) - P_2^3 = G(\tilde{c}_3) - P_1^3\} \\
&\quad \leq (L_E(\Gamma_{c_\epsilon}))^2 + \epsilon D(\Gamma_{c_\epsilon}) \leq C_0.
\end{aligned}$$

In the next step we would like to send the parameter ϵ to zero. To that end, using the quasinormality of the minima, we first observe that

$$\begin{aligned}
(2+\epsilon)D(\Gamma_{c_\epsilon}) &= (\sum_{\alpha=1}^{3} \int_0^1 |(c_\epsilon)_u|^2 du) + \epsilon D(\Gamma_{c_\epsilon}) = (\sum_{\alpha=1}^{3} |(c_\epsilon)_u|^2) + \epsilon D(\Gamma_{c_\epsilon}) \\
&\leq (\sum_{\alpha=1}^{3} |(c_\epsilon)_u|)^2 + \epsilon D(\Gamma_{c_\epsilon}) = (\sum_{\alpha=1}^{3} \int_0^1 |(c_\epsilon)_u| du)^2 + \epsilon D(\Gamma_{c_\epsilon}) \\
&= (L_E(\Gamma_{c_\epsilon}))^2 + \epsilon D(\Gamma_{c_\epsilon}) \leq C_0,
\end{aligned}$$

from which we infer that

$$D(\Gamma_{c_\epsilon}) \leq C_0 \tag{3.4}$$

for all $0 < \epsilon \leq 1$. Using the quasinormality we even have

$$|(c_{\epsilon,\alpha})_u|^2 = constant \leq 2C_0 \tag{3.5}$$

for all $0 < \epsilon \leq 1$ and $\alpha = 1,2,3$. Repeating the same argument as above (cf. (3.3)), replacing Γ_{c_n} with Γ_{c_ϵ}, we obtain

$$\|c_{\epsilon,\alpha}\|_{H^{1,2}(0,1)} \leq C \text{ for any } 0 < \epsilon < 1,\ \alpha = 1,2,3,$$

for a constant C independent of ϵ. Moreover, for any $u_1, u_2 \in [0,1]$, $u_1 \leq u_2$, we have (using (3.5))

$$|c_{\epsilon,\alpha}(u_2) - c_{\epsilon,\alpha}(u_1)| \leq \int_{u_1}^{u_2} |\partial_u(c_{\epsilon,\alpha})| du = |(c_{\epsilon,\alpha})_u||u_1 - u_2| \leq C|u_1 - u_2| \quad \alpha = 1,2,3,$$

and for all $\epsilon \in (0,1)$. Again using the Theorem of Ascoli–Arzelà we infer the existence of

$$\Gamma_c \in \mathcal{C}_D \cap C^{0,1}([0,1])$$

to which a subsequence of Γ_{c_ϵ} converges uniformly on $[0,1]$ as well as weakly in $H^{1,2}(0,1)$. The triod Γ_c satisfies also the integral constraints given in (3.2).

Observe that

$$\begin{aligned}
0 \leq d :&= \inf\{(L_E(\Gamma_{\tilde{c}}))^2 \,:\, \Gamma_{\tilde{c}} \in \mathcal{C}_D, \quad G(\tilde{c}_1) - P_1^3 = G(\tilde{c}_2) - P_2^3 = G(\tilde{c}_3) - P_1^3\} \\
&\leq \inf\{(L_E(\Gamma_{\tilde{c}}))^2 + \epsilon D(\Gamma_{\tilde{c}}) \,:\, \Gamma_{\tilde{c}} \in \mathcal{C}_D, \quad G(\tilde{c}_1) - P_1^3 = G(\tilde{c}_2) - P_2^3 = G(\tilde{c}_3) - P_1^3\} \\
&= (L_E(\Gamma_{c_\epsilon}))^2 + \epsilon D(\Gamma_{c_\epsilon}) =: d(\epsilon).
\end{aligned}$$

Since the map $[0,1] \ni \epsilon \mapsto d(\epsilon)$ is non decreasing, it has a limit as ϵ goes to zero and there holds

$$d \leq \lim_{\epsilon \to 0} d(\epsilon).$$

On the other hand, using (3.4), we obtain for the limit of $d(\epsilon)$ that

$$\lim_{\epsilon \to 0} d(\epsilon) = \lim_{\epsilon \to 0} (L_E(\Gamma_{c_\epsilon}))^2 + \epsilon D(\Gamma_{c_\epsilon}) = \lim_{\epsilon \to 0} (L_E(\Gamma_{c_\epsilon}))^2. \tag{3.6}$$

Taking a sequence $\epsilon_j \to 0$ for which $\Gamma(c_{\epsilon_j})$ converges weakly to Γ_c in $H^{1,2}(0,1)$ we infer using the sequentially weak lower semicontinuity of the length functional that

$$d \leq (L_E(\Gamma_c))^2 \leq \liminf_{\epsilon_j \to 0} (L_E(\Gamma_{c_{\epsilon_j}}))^2 = \lim_{\epsilon \to 0} (L_E(\Gamma_{c_\epsilon}))^2. \tag{3.7}$$

On the other hand, using the minimality of Γ_{c_ϵ}, we can write

$$(L_E(\Gamma_{c_\epsilon}))^2 + \epsilon D(\Gamma_{c_\epsilon}) \leq (L_E(\Gamma_c))^2 + \epsilon D(\Gamma_c),$$

so that

$$\lim_{\epsilon \to 0} d(\epsilon) = \lim_{\epsilon \to 0} (L_E(\Gamma_{c_\epsilon}))^2 + \epsilon D(\Gamma_{c_\epsilon}) \leq (L_E(\Gamma_c))^2. \tag{3.8}$$

From (3.7), (3.6), (3.8) we therefore obtain that

$$d \leq (L_E(\Gamma_c))^2 \leq \lim_{\epsilon \to 0} (L_E(\Gamma_{c_\epsilon}))^2 = \lim_{\epsilon \to 0} d(\epsilon) \leq (L_E(\Gamma_c))^2,$$

so that

$$d \leq (L_E(\Gamma_c))^2 = \lim_{\epsilon \to 0} d(\epsilon). \tag{3.9}$$

On the other hand since $d(\epsilon) \leq (L_E(\Gamma_{\hat{c}}))^2 + \epsilon D(\Gamma_{\hat{c}})$ for any admissible $\Gamma_{\hat{c}} \in \mathcal{C}_D$ satisfying the constraints given in (3.2), we also have that

$$\lim_{\epsilon \to 0} d(\epsilon) \leq (L_E(\Gamma_{\hat{c}}))^2 \quad \forall\, \Gamma_{\hat{c}} \in \mathcal{C}_D \text{ satisfying the constraints.}$$

Hence

$$\lim_{\epsilon \to 0} d(\epsilon) \leq d = \inf\{(L_E(\Gamma_{\tilde{c}}))^2 \,:\, \Gamma_{\tilde{c}} \in \mathcal{C}_D, \quad G(\tilde{c}_1) - P_1^3 = G(\tilde{c}_2) - P_2^3 = G(\tilde{c}_3) - P_1^3\}. \tag{3.10}$$

From (3.9) and (3.10) we finally infer that

$$d = (L_E(\Gamma_c))^2 = \lim_{\epsilon \to 0} d(\epsilon),$$

in other words

$$(L_E(\Gamma_c))^2 = \inf\{(L_E(\Gamma_{\tilde{c}}))^2 \,:\, \Gamma_{\tilde{c}} \in \mathcal{C}_D, \quad G(\tilde{c}_1) - P_1^3 = G(\tilde{c}_2) - P_2^3 = G(\tilde{c}_3) - P_1^3\}.$$

It then follows that the triod $\Gamma_c \in \mathcal{C}_D \cap C^{0,1}([0,1])$ realizes also the following minimum problem

$$L_E(\Gamma_c) = \inf\{L_E(\Gamma_{\tilde{c}}) \,:\, \Gamma_{\tilde{c}} \in \mathcal{C}_D, \quad G(\tilde{c}_1) - P_1^3 = G(\tilde{c}_2) - P_2^3 = G(\tilde{c}_3) - P_1^3\}, \tag{3.11}$$

as well as

$$\begin{aligned} L_E(\Gamma_c) &= \inf\{L_E(\Gamma_{\tilde{c}}) \,:\, \Gamma_{\tilde{c}} \in \mathcal{C}_D, \quad G(\tilde{c}_1) - P_1^3 = G(\tilde{c}_2) - P_2^3 = G(\tilde{c}_3) - P_1^3\} \\ &= \inf\{L_E(\Gamma_{\tilde{c}}) \,:\, \Gamma_{\tilde{c}} \in \mathcal{C}_D \cap C^{0,1}([0,1]), \quad G(\tilde{c}_1) - P_1^3 = G(\tilde{c}_2) - P_2^3 = G(\tilde{c}_3) - P_1^3\} \\ &= \inf\{L_E(\Gamma_{\tilde{c}}) \,:\, \Gamma_{\tilde{c}} \in \mathcal{C} \cap C^{0,1}([0,1]), \quad G(\tilde{c}_1) - P_1^3 = G(\tilde{c}_2) - P_2^3 = G(\tilde{c}_3) - P_1^3\}. \end{aligned}$$

3.2 Euler–Lagrange equations and regularity of minimizers

For simplicity of exposition later on, let us first remark that quasinormal critical points for a linear combination of the functionals L_E and G are automatically smooth.

Lemma 3.1. *Let $\lambda \in \mathbb{R}$ and let $c \in C^{0,1}([0,1], \mathbb{R}^2)$ be a quasinormal curve satisfying*

$$\frac{d}{d\epsilon}\Big|_{\epsilon=0} (L_E(c + \epsilon\phi) + \lambda G(c + \epsilon\phi)) = \delta L_E(c)\phi + \lambda \delta G(c)\phi = 0 \qquad \forall\, \phi \in C_0^\infty((0,1), \mathbb{R}^2).$$

Then $c \in C^\infty([0,1], \mathbb{R}^2)$.

Proof. Recalling (2.13) we have that

$$0 = \int_0^1 \frac{c_u}{|c_u|} \cdot \phi_u du + \lambda \int_0^1 \begin{pmatrix} \phi^1 \\ \phi^2 \end{pmatrix} \cdot \begin{pmatrix} c_u^2 \\ -c_u^1 \end{pmatrix} du \qquad \forall\, \phi \in C_0^\infty((0,1),\mathbb{R}^2). \tag{3.12}$$

Since $|c_u| = L_E(c) > 0$ by assumption we obtain for each space component $j = 1, 2$ that

$$\left| \int_0^1 \partial_u c^j \, \partial_u \phi \, du \right| \le C(c,\lambda) \|\phi\|_{L^2(0,1)} \qquad \forall\, \phi \in C_0^\infty((0,1),\mathbb{R}),$$

yielding $c \in H^{2,2}((0,1),\mathbb{R}^2)$ by the characterization of Sobolev spaces (see for instance [6, Theorem 2.9]). Then, integrating by parts in (3.12) and using the fundamental lemma of calculus of variation we infer (writing $ds = L_E(c)du$ for the length element) that

$$\partial_{ss} c^1 = \lambda c_s^2, \qquad \partial_{ss} c^2 = -\lambda c_s^1$$

and a boot-strap argument yields the claim. □

Remark 3.2. *Even without having calculated the Euler–Lagrange equation yet, we may have already some intuition about the shape of minimal triods. Let $\Gamma_c \in \mathcal{C}_D \cap C^{0,1}([0,1])$ be a minimizer satisfying (3.11) and let $\Gamma = (\gamma_1, \gamma_2, \gamma_3)$ be its horizontal lift (with each curve c_α lifted to a horizontal curve γ_α ending at P_α, $\alpha = 1, 2, 3$).*

Without loss of generality, i.e. after an appropriate left translation of Γ, we might assume that the junction point Σ coincides with the origin (recall Remark 2.5). Moreover, let us still denote by P_α the translated endpoints.

We immediately observe that if the points P_α lie in the (x, y)-plane, i.e. $P_\alpha^3 = 0$ for any $\alpha = 1, 2, 3$, then, since the shortest path between P_α and $\Sigma = 0$ is a straight line, our minimal triod Γ must be a solution of the classical Steiner problem. This means that if the largest angle of the triangle with vertices given by the P_α is larger than or equal to 120 degrees, then Σ coincides with the vertex of the largest angle. Otherwise Σ is a point distinct from the points P_α and the three lines meet in Σ at an angle of 120 degrees (see for example [15, §5]).

On the other hand, if at least one of the points P_α does not lie in the (x, y)-plane, then the situation is not so clear anymore. But (in view of Remark 2.12 and Remark A.2) it is reasonable to believe that the projection of a minimal configuration Γ_c will be composed of arcs of circles and/or straight segments.

In the following let $\Gamma_c \in \mathcal{C}_D \cap C^{0,1}([0,1])$ be a minimizer satisfying (3.11) and let $\Gamma = (\gamma_1, \gamma_2, \gamma_3)$ be its horizontal lift (with each curve c_α lifted to a horizontal curve γ_α ending at P_α, $\alpha = 1, 2, 3$). For simplicity of exposition we assume here that the triod is not degenerate, i.e. no curves have collapsed to a point.

Upon a suitable reparametrization ([6, Lemma 5.23]), we may assume furthermore that the triod is quasinormal (according to Definition 3.1).

To calculate the Euler–Lagrange equations denote by

$$\mathcal{T} := \{\Phi = (\phi_1, \phi_2, \phi_3) \,:\, \phi_\alpha \in C^\infty([0,1],\mathbb{R}^2), \phi_\alpha(1) = (0,0)^t, \alpha = 1,2,3, \quad \phi_1(0) = \phi_2(0) = \phi_3(0)\}$$

the space of test functions, and by

$$\begin{aligned} \mathcal{G}_1(\Gamma_{\tilde{c}}) &:= G(\tilde{c}_1) - G(\tilde{c}_2) - P_1^3 + P_2^3, \\ \mathcal{G}_2(\Gamma_{\tilde{c}}) &:= G(\tilde{c}_2) - G(\tilde{c}_3) - P_2^3 + P_1^3, \end{aligned}$$

the two constraints given in (3.11). Choose $\varphi_i \in C_0^\infty((0,1),\mathbb{R}^2)$, $i = 1, 3$, such that

$$0 \neq \delta G(c_i)(\varphi_i) = \int_0^1 \begin{pmatrix} \varphi_i^1 \\ \varphi_i^2 \end{pmatrix} \cdot \begin{pmatrix} (c_i^2)_u \\ -(c_i^1)_u \end{pmatrix} du$$

(which exists thanks to the regularity of the curves c_i) and set

$$\Phi_1 := (\varphi_1, 0, 0), \qquad \Phi_3 := (0, 0, \varphi_3).$$

Next, for $\Phi \in \mathcal{T}$, consider the map

$$\mathbb{R}^3 \ni (\epsilon, t_1, t_2)^t \mapsto \mathcal{G}(\epsilon, t_1, t_2) := \begin{pmatrix} \mathcal{G}_1(\Gamma_c + \epsilon\Phi + t_1\Phi_1 + t_2\Phi_3) \\ \mathcal{G}_2(\Gamma_c + \epsilon\Phi + t_1\Phi_1 + t_2\Phi_3) \end{pmatrix} = \begin{pmatrix} \mathcal{G}_1(\Gamma_c + \epsilon\Phi + t_1\Phi_1) \\ \mathcal{G}_2(\Gamma_c + \epsilon\Phi + t_2\Phi_3) \end{pmatrix},$$

where in the last equality we have used the definition of $\mathcal{G}_i$, $i = 1, 2$. Note also that the triod $\Gamma_c + \epsilon\Phi + t_1\Phi_1 + t_2\Phi_3$ belongs to $\mathcal{C}_D$ for any choice of ϵ, t_1, t_2.

We have $\mathcal{G}(0, 0, 0) = (0, 0)^t$ by assumption and

$$\frac{\partial \mathcal{G}}{\partial t}(0) := \frac{\partial \mathcal{G}}{\partial(t_1, t_2)}(0, 0, 0) = \begin{pmatrix} \delta G(c_1)(\varphi_1) & 0 \\ 0 & -\delta G(c_3)(\varphi_3) \end{pmatrix}$$

has maximal rank. By the implicit function theorem we can find C^1-maps σ_r, $r = 1, 2$, defined in a neighbourhood of zero such that $\sigma_r(0) = 0$ and

$$\mathcal{G}(\epsilon, \sigma_1(\epsilon), \sigma_2(\epsilon)) = (0, 0)^t, \qquad \text{for } \epsilon \in (-\epsilon_0, \epsilon_0), \tag{3.13}$$

which implies that $\Gamma_c + \epsilon\Phi + \sigma_1(\epsilon)\Phi_1 + \sigma_2(\epsilon)\Phi_3$ is an admissible variation for any $\epsilon \in (-\epsilon_0, \epsilon_0)$. Differentiation of the above system (3.13) yields

$$\begin{pmatrix} \sigma_1'(0) \\ \sigma_2'(0) \end{pmatrix} = -(\frac{\partial \mathcal{G}}{\partial t}(0))^{-1} \begin{pmatrix} \delta\mathcal{G}_1(\Gamma_c)\Phi \\ \delta\mathcal{G}_2(\Gamma_c)\Phi \end{pmatrix}.$$

From the minimality of Γ_c we infer

$$0 = \frac{d}{d\epsilon}\Big|_{\epsilon=0} L_E(\Gamma_c + \epsilon\Phi + \sigma_1(\epsilon)\Phi_1 + \sigma_2(\epsilon)\Phi_3) = \delta L_E(\Gamma_c)\Phi + \sigma_1'(0)\delta L_E(\Gamma_c)\Phi_1 + \sigma_2'(0)\delta L_E(\Gamma_c)\Phi_3$$

and substituting the values for $\sigma_r'(0)$ we finally infer that there exists Lagrange multipliers $\lambda_j \in \mathbb{R}$, $j = 1, 2$, such that

$$0 = \frac{d}{d\epsilon}\Big|_{\epsilon=0} \left(L_E(\Gamma_c + \epsilon\Phi) + \sum_{j=1}^{2} \lambda_j \mathcal{G}_j(\Gamma_c + \epsilon\Phi) \right)$$

for any $\phi \in \mathcal{T}$. In other words, for any $\Phi = (\phi_1, \phi_2, \phi_3) \in \mathcal{T}$ we have that

$$0 = \sum_{i=1}^{3} \delta L_E(c_i)\phi_i + \lambda_1 \delta G(c_1)\phi_1 - \lambda_2 \delta G(c_3)\phi_3 + (\lambda_2 - \lambda_1)\delta G(c_2)\phi_2. \tag{3.14}$$

This yields that

$$0 = \delta L_E(c_1)\phi + \lambda_1 \delta G(c_1)\phi, \tag{3.15a}$$
$$0 = \delta L_E(c_2)\phi + (\lambda_2 - \lambda_1)\delta G(c_2)\phi, \tag{3.15b}$$
$$0 = \delta L_E(c_3)\phi - \lambda_2 \delta G(c_3)\phi, \tag{3.15c}$$

for any $\varphi \in C_0^\infty((0, 1), \mathbb{R}^2)$, which in turns yields that the curves are smooth thanks to Lemma 3.1 and (recalling the computations performed in Remark 2.12) that the curvatures k_α of the three curves c_α are constant and equal to:

$$\begin{aligned} &k_1(u) + \lambda_1 = 0 \quad \text{for } u \in (0, 1), \\ &k_2(u) + (\lambda_2 - \lambda_1) = 0 \quad \text{for } u \in (0, 1), \\ &k_3(u) - \lambda_2 = 0 \quad \text{for } u \in (0, 1), \end{aligned}$$

in other words

$$\sum_{\alpha=1}^{3} k_\alpha = 0. \tag{3.16}$$

Further we infer from (3.14) (considering now test functions $\Phi \in \mathcal{T}$ that do not vanish near the triple junction so that we may retrieve the natural boundary conditions, using (3.15), and recalling (2.13)) that

$$0 = \sum_{\alpha=1}^{3} \left[\begin{pmatrix} \phi_\alpha^1 \\ \phi_\alpha^2 \end{pmatrix} \cdot \begin{pmatrix} (c_\alpha^1)_u \\ (c_\alpha^2)_u \end{pmatrix} \frac{1}{|(c_\alpha)_u|} \right]_0^1$$

$$
\begin{aligned}
&+\frac{\lambda_1}{2}\left[\begin{pmatrix}\phi_1^1\\ \phi_1^2\end{pmatrix}\cdot\begin{pmatrix}-c_1^2\\ c_1^1\end{pmatrix}\right]_0^1+\frac{\lambda_2-\lambda_1}{2}\left[\begin{pmatrix}\phi_2^1\\ \phi_2^2\end{pmatrix}\cdot\begin{pmatrix}-c_2^2\\ c_2^1\end{pmatrix}\right]_0^1-\frac{\lambda_2}{2}\left[\begin{pmatrix}\phi_3^1\\ \phi_3^2\end{pmatrix}\cdot\begin{pmatrix}-c_3^2\\ c_3^1\end{pmatrix}\right]_0^1\\
&=-\phi_1(0)\cdot\left\{\left(\sum_{\alpha=1}^{3}\begin{pmatrix}(c_\alpha^1)_u\\ (c_\alpha^2)_u\end{pmatrix}\frac{1}{|(c_\alpha)_u|}\right)+\frac{\lambda_1}{2}\begin{pmatrix}-c_1^2\\ c_1^1\end{pmatrix}+\frac{\lambda_2-\lambda_1}{2}\begin{pmatrix}-c_2^2\\ c_2^1\end{pmatrix}-\frac{\lambda_2}{2}\begin{pmatrix}-c_3^2\\ c_3^1\end{pmatrix}\right\}\Big|_{u=0}\\
&=-\phi_1(0)\cdot\left\{\left(\sum_{\alpha=1}^{3}\begin{pmatrix}(c_\alpha^1)_u\\ (c_\alpha^2)_u\end{pmatrix}\frac{1}{|(c_\alpha)_u|}\right)\right\}\Big|_{u=0},
\end{aligned}
$$

where we have used the facts that $\phi_1(0)=\phi_2(0)=\phi_3(0)$ and $c_1(0)=c_2(0)=c_3(0)$. In particular, we infer that the projected curves meet at the projected triple junction at angles of 120 degrees, i.e.

$$
0=\sum_{\alpha=1}^{3}\begin{pmatrix}(c_\alpha^1)_u\\ (c_\alpha^2)_u\end{pmatrix}\frac{1}{|(c_\alpha)_u|}\Big|_{u=0}=\sum_{\alpha=1}^{3}\frac{(c_\alpha)_u}{|(c_\alpha)_u|}\Big|_{u=0}. \tag{3.17}
$$

Remark 3.3. *If the minimal triod Γ is degenerate, we can repeat the above arguments with $P_2=\Sigma$, $G(c_2)=0$, i.e. with $c_2([0,1])=\overline{P}_2$. Then the integral constraints become*

$$
P_2^3=P_1^3-G(\tilde{c}_1)=P_3^3-G(\tilde{c}_3)
$$

(which are essentially decoupled), providing the existence of some $\lambda_1,\lambda_2\in\mathbb{R}$ for which

$$
\begin{aligned}
0&=\delta L_E(c_1)\phi+\lambda_1\delta G(c_1)\phi,\\
0&=\delta L_E(c_3)\phi-\lambda_2\delta G(c_3)\phi.
\end{aligned}
$$

for any $\varphi\in C_0^\infty((0,1),\mathbb{R}^2)$, so that

$$
k_1+\lambda_1=0=k_3-\lambda_2 \text{ on } [0,1].
$$

Remark 3.4. *From* (3.16) *we infer that for a non-degenerate minimal triod Γ_c (or more generally a non-degenerate solution of the Euler–Lagrange equation* (3.14)*) the following situations can occur:*

(i) $k_1=k_2=0\Rightarrow k_3=0$, *i.e. three straight segments meet at 120 degree angles;*

(ii) $k_1=0$, $k_2=-k_3\neq 0$, *i.e. one straight segment and two arcs of curvature equal in absolute value meet at a projected angles of 120 degrees;*

(iii) $k_1,k_2,k_3\neq 0$ *and* (3.16), (3.17) *hold.*

Again let $\Gamma=(\gamma_1,\gamma_2,\gamma_3)$ be the horizontal lift of Γ_c (with each curve c_α lifted to a horizontal curve γ_α ending at P_α, $\alpha=1,2,3$). A Steiner minimal configuration of type (i) is given for example by connecting through straight lines the junction point $\Sigma=0$ with $P_1=(1,0,0)^t$, $P_2=(\cos(2\pi/3),\sin(2\pi/3),0)^t=(-\frac{\sqrt{3}}{2},\frac{1}{2},0)^t$, and $P_3=(\cos(-2\pi/3),\sin(-2\pi/3),0)^t=(-\frac{\sqrt{3}}{2},-\frac{1}{2},0)^t$ (cf. also Experiment 1 in Section 5).

A critical configuration of type (ii) can be constructed, for instance, by modifying the previous example as follows: we take the junction point $\Sigma=0$ to be connected with a straight line with $P_1=(1,0,0)^t$ (here $\lambda_1=0$). The two remaining points P_2 and P_3 shall now not lie in the (x,y)-plane. To construct two horizontal geodesics meeting in Σ at the right angle (and parametrized by arc length with $L_E(c_i)=s_f=1$ for simplicity) we use Remark A.2. For the curve c_2 connecting the origin to P_2, take for instance (using the notation adopted in Remark A.2) $c_2(0)=0$, $|B|=1$, $\alpha_0=\frac{2}{3}\pi$, so that by (A.7), (A.6) *with $\lambda_2=\pi$*

$$
P_2^3=-\frac{1}{2\lambda}=-\frac{1}{2\pi},\qquad \gamma_2^3(s)=-\frac{1}{2\pi}s+\frac{1}{2\pi^2}\sin(\pi s),\quad s\in[0,1].
$$

More precisely, the curve $c_2:[0,1]\to\mathbb{R}^2$ is parametrized by

$$
c_2(s)=\frac{1}{\pi}\begin{pmatrix}\sin(\frac{2\pi}{3})\\ -\cos(\frac{2\pi}{3})\end{pmatrix}+\frac{1}{\pi}\begin{pmatrix}\sin(\pi s-\frac{2\pi}{3})\\ \cos(\pi s-\frac{2\pi}{3})\end{pmatrix},\quad s\in[0,1].
$$

For the curve c_3 connecting the origin Σ to P_3, we obtain with $c_3(0) = 0$, $|B| = 1$, $\alpha_0 = -\frac{2}{3}\pi$,$s_f = 1$, $\lambda = -\pi$

$$P_3^3 = -\frac{1}{2\lambda} = +\frac{1}{2\pi}, \qquad \gamma_3^3(s) = \frac{1}{2\pi}s + \frac{1}{2\pi^2}\sin(-\pi s), \quad s \in [0,1].$$

More precisely, the curve $c_3 : [0,1] \to \mathbb{R}^2$ is parametrized by

$$c_3(s) = \frac{1}{\pi}\begin{pmatrix}\sin(\frac{2\pi}{3})\\ \cos(\frac{2\pi}{3})\end{pmatrix} + \frac{1}{\pi}\begin{pmatrix}\sin(\pi s - \frac{2\pi}{3})\\ -\cos(\pi s - \frac{2\pi}{3})\end{pmatrix}, \quad s \in [0,1].$$

Further critical configurations of type (ii) are retrieved numerically for instance in Experiments 2 and 5 in Section 5. Critical configurations of type (iii) are shown for instance in Experiments 11 and 13.

3.3 Formulation of horizontal curve shortening flow for triods

Similarly to what is discussed in Appendix B, we can provide here evolution problems whose stationary solutions yield critical points for the functional L as given in (3.1). The following formulations are at the basis of the numerical schemes and simulations proposed in Section 4 and 5.

Assumption 3.5. *Let $P_1, P_2, P_3 \in \mathbb{R}^3$ be three given distinct points and let $\gamma_{0,\alpha} : [0,1] \to \mathbb{R}^3$, $\alpha = 1,2,3$, be regular smooth horizontal curves such that*

$$\gamma_{0,\alpha}(1) = P_\alpha, \qquad \alpha = 1,2,3,$$
$$\gamma_{0,1}(0) = \gamma_{0,2}(0) = \gamma_{0,3}(0).$$

Our aim now is to let such an initial triod evolve in time in such a way that its flow converges to critical points of L. Since the junction point must be able to move in time, tangential movements must be allowed. Recalling (2.10) we formulate:

Problem 3.6. *Let Assumption 3.5 hold (together with appropriate compatibility conditions). Find $\Gamma = (\gamma_1, \gamma_2, \gamma_3)$ with $\gamma_\alpha : [0,T) \times [0,1] \to \mathbb{R}^3$, $\gamma_\alpha = \gamma_\alpha(t,u)$, $\alpha = 1,2,3$ (in an appropriate class of functions), which satisfies $\gamma_\alpha(0,\cdot) = \gamma_{0,\alpha}(\cdot)$, and*

$$\begin{aligned}
\partial_t \gamma_1^{\perp_g}(t,u) &= \vec{k}_{1,g}(t,u) + \lambda_1(t)N_1(t,u) + \Big(\int_u^1 (k_1(t,\xi) + \lambda_1(t))|\partial_u\gamma_1(t,\xi)|_g d\xi\Big)X_3(\gamma_1(t,u)),\\
\partial_t \gamma_2^{\perp_g}(t,u) &= \vec{k}_{2,g}(t,u) + (\lambda_2(t) - \lambda_1(t))N_2(t,u)\\
&\quad + \Big(\int_u^1 (k_2(t,\xi) + \lambda_2(t) - \lambda_1(t))|\partial_u\gamma_2(t,\xi)|_g d\xi\Big)X_3(\gamma_2(t,u)),\\
\partial_t \gamma_3^{\perp_g}(t,u) &= \vec{k}_{3,g}(t,u) - \lambda_2(t)N_3(t,u) + \Big(\int_u^1 (k_3(t,\xi) - \lambda_2(t))|\partial_u\gamma_3(t,\xi)|_g d\xi\Big)X_3(\gamma_3(t,u)),\\
\gamma_1(t,0) &= \gamma_2(t,0) = \gamma_3(t,0) \quad \text{for all } t \in (0,T),\\
\gamma_\alpha(t,1) &= P_\alpha \quad \text{for all } t \in (0,T), \quad \alpha = 1,2,3,\\
0 &= \sum_{\alpha=1}^3 \begin{pmatrix}(\gamma_\alpha^1)_u(t,u)\\ (\gamma_\alpha^2)_u(t,u)\end{pmatrix} \frac{1}{|\partial_u\gamma_\alpha(t,u)|_g}\Big|_{u=0} \text{ for all } t \in [0,T],
\end{aligned}$$

where the Lagrange multipliers are given through (3.19), below, for the projected curves c_α. Here $\partial_t\gamma_\alpha^{\perp_g}$ is short for $\partial_t\gamma_\alpha^{\perp_g} := \partial_t\gamma_\alpha - g(\partial_t\gamma_\alpha, T_\alpha)T_\alpha$.

If $\Gamma = (\gamma_1, \gamma_2, \gamma_3)$ is a solution to Problem 3.6, then its projected triod $\Gamma_c = (c_1, c_2, c_3)$, with $c_\alpha = (\gamma_\alpha^1, \gamma_\alpha^2)^t$, $\alpha = 1,2,3$, satisfies the following problem in the Euclidean setting.

Problem 3.7. *Let Assumption 3.5 hold (together with appropriate compatibility conditions). Find $\Gamma_c = (c_1, c_2, c_3)$, with $c_\alpha : [0,T) \times [0,1] \to \mathbb{R}^2$, $c_\alpha = (\gamma_\alpha^1, \gamma_\alpha^2)^t$, $\alpha = 1,2,3$, (in an appropriate class of functions), which satisfies $\gamma_\alpha^r(0,\cdot) = \gamma_{0,\alpha}^r$ for $r = 1,2$, $\alpha = 1,2,3$, and*

$$(\partial_t c_1 \cdot \vec{n}_1)\vec{n}_1 = \vec{k}_1 + \lambda_1(t)\vec{n}_1 \qquad \text{for } (t,u) \in (0,T) \times (0,1), \tag{3.18a}$$

$$(\partial_t c_2 \cdot \vec{n}_2)\vec{n}_2 = \vec{k}_2 + (\lambda_2(t) - \lambda_1(t))\vec{n}_2 \qquad \textit{for } (t,u) \in (0,T) \times (0,1), \tag{3.18b}$$

$$(\partial_t c_3 \cdot \vec{n}_3)\vec{n}_3 = \vec{k}_3 - \lambda_2(t)\vec{n}_3 \qquad \textit{for } (t,u) \in (0,T) \times (0,1), \tag{3.18c}$$

$$c_\alpha(t,1) = (P^1_\alpha, P^2_\alpha)^t \qquad \textit{for all } t \in [0,T), \tag{3.18d}$$

$$c_1(t,0) = c_2(t,0) = c_3(t,0) \qquad \textit{for all } t \in (0,T), \tag{3.18e}$$

$$0 = \sum_{\alpha=1}^{3} \frac{\partial_u c_\alpha}{|\partial_u c_\alpha|}\Big|_{u=0} \qquad \textit{for all } t \in (0,T), \tag{3.18f}$$

where

$$\vec{n}_\alpha := \frac{1}{|\partial_u c_\alpha|}\begin{pmatrix} -\partial_u \gamma^2_\alpha(t,u) \\ \partial_u \gamma^1_\alpha(t,u) \end{pmatrix}, \qquad I_K(c_\alpha(t)) := \int_0^1 k_\alpha(t,u)|\partial_u c_\alpha| du, \qquad \alpha = 1,2,3,$$

and the Lagrange multipliers λ_1, λ_2 are solutions of

$$\begin{pmatrix} L_E(c_1(t)) + L_E(c_2(t)) & -L_E(c_2(t)) \\ -L_E(c_2(t)) & L_E(c_3(t)) + L_E(c_2(t)) \end{pmatrix}\begin{pmatrix} \lambda_1(t) \\ \lambda_2(t) \end{pmatrix} = \begin{pmatrix} I_K(c_2(t)) - I_K(c_1(t)) \\ I_K(c_3(t)) - I_K(c_1(t)) \end{pmatrix}. \tag{3.19}$$

Note that the Lagrange multipliers are well defined as long as the lengths of at least two curves are not zero, and that if $L_E(c_2) = 0$ then the system decouples into two fully independent equations with Lagrange multipliers that are computed as in Problem B.2.

Lemma 3.8. *For a (sufficiently smooth) solution to Problem 3.7 we have that*

$$\frac{d}{dt}\sum_{\alpha=1}^{3} L_E(c_\alpha(t)) \le 0.$$

Proof. First of all recall that for a planar curve $c = (c^1, c^2)^t = (\gamma^1, \gamma^2)^t$ such that $c(t,1)$ is a fixed point and $c(t,0)$ a mobile one, we have (recall (2.12))

$$\frac{d}{dt}G(c) = -\int_0^1 c_t \cdot \vec{n}|c_u| du - \frac{1}{2}[c_t \cdot c^\perp]_{u=0}.$$

Note that for the lifted curve γ (recall (2.2)) with $\gamma(t,1)$ a fixed point and $\gamma(t,0)$ a mobile one, the above equation implies

$$-\partial_t \gamma^3(t,0) = \frac{d}{dt}(\gamma^3(t,1) - \gamma^3(t,0)) = \frac{d}{dt}G(c) = -\int_0^1 c_t \cdot \vec{n}|c_u| du - \frac{1}{2}[c_t \cdot c^\perp]_{u=0}. \tag{3.20}$$

Using $c_1(t,0) = c_2(t,0) = c_3(t,0)$ it follows then that

$$\frac{d}{dt}G(c_\alpha) = \frac{d}{dt}G(c_\beta) \iff \int_0^1 \partial_t c_\alpha \cdot \vec{n}_\alpha |\partial_u c_\alpha| du = \int_0^1 \partial_t c_\beta \cdot \vec{n}_\beta |\partial_u c_\beta| du \qquad \text{for } \alpha, \beta \in \{1,2,3\}. \tag{3.21}$$

A straightforward calculation yields then that

$$\int_0^1 \partial_t c_1 \cdot \vec{n}_1 |\partial_u c_1| du = \int_0^1 \partial_t c_2 \cdot \vec{n}_2 |\partial_u c_2| du = \int_0^1 \partial_t c_3 \cdot \vec{n}_3 |\partial_u c_3| du \quad \iff \quad \text{(3.19) holds.} \tag{3.22}$$

Now that the effect of the choice of the Lagrange multipliers is clarified, we can compute

$$\begin{aligned}
\frac{d}{dt}\sum_{\alpha=1}^{3} L_E(c_\alpha(t)) &= \sum_{\alpha=1}^{3}\left[\frac{\partial_u c_\alpha}{|\partial_u c_\alpha|} \cdot \partial_t c_\alpha\right]_0^1 - \sum_{\alpha=1}^{3}\int_0^1 \vec{k}_\alpha \cdot \partial_t c_\alpha |\partial_u c_\alpha| du \\
&= -\sum_{\alpha=1}^{3}\int_0^1 \vec{k}_\alpha \cdot (\partial_t c_\alpha \cdot \vec{n}_\alpha)\vec{n}_\alpha |\partial_u c_\alpha| du \\
&= -\left(\sum_{\alpha=1}^{3}\int_0^1 |(\partial_t c_\alpha \cdot \vec{n}_\alpha)\vec{n}_\alpha|^2 |\partial_u c_\alpha| du\right) + \lambda_1(t)\int_0^1 \partial_t c_1 \cdot \vec{n}_1 |\partial_u c_1| du
\end{aligned}$$

$$
\begin{aligned}
&+ (\lambda_2(t) - \lambda_1(t)) \int_0^1 \partial_t c_2 \cdot \vec{n}_2 |\partial_u c_2| du - \lambda_2(t) \int_0^1 \partial_t c_3 \cdot \vec{n}_3 |\partial_u c_3| du \\
&= - \sum_{\alpha=1}^{3} \int_0^1 |(\partial_t c_\alpha \cdot \vec{n}_\alpha)\vec{n}_\alpha|^2 |\partial_u c_\alpha| du \leq 0,
\end{aligned}
$$

where we have used the boundary conditions and (3.22). □

From the above lemma we immediately infer that for a solution of Problem 3.6 the length decreases along the flow since (recall Remark 2.1)

$$
\frac{d}{dt} L(\Gamma(t)) = \frac{d}{dt} \left(\sum_{\alpha=1}^{3} L_E(c_\alpha(t)) \right) \leq 0.
$$

With similar considerations explained in Section B, and using (3.21), (3.20), (2.2), and Assumption 3.5, one can show that a horizontal lift of a solution Γ_c to Problem 3.7, where each curve c_α is lifted to a horizontal curve γ_α ending at P_α, yields a solution to Problem 3.6. More precisely for a lifted curve γ we observe by differentiating in time (2.2) that

$$
\begin{aligned}
\partial_t \gamma^3(t,u) &= \partial_t \gamma^3(t,0) + \int_0^u \left(-\frac{1}{2}\gamma_t^2 \gamma_u^1 - \frac{1}{2}\gamma^2 \gamma_{tu}^1 + \frac{1}{2}\gamma_t^1 \gamma_u^2 + \frac{1}{2}\gamma^1 \gamma_{tu}^2 \right) d\xi \\
&= \partial_t \gamma^3(t,0) + \int_0^u \left(-\gamma_t^2 \gamma_u^1 + \gamma_t^1 \gamma_u^2 \right) d\xi + [\frac{1}{2}\gamma^1 \gamma_t^2 - \frac{1}{2}\gamma^2 \gamma_t^1]_0^u \\
&= \partial_t \gamma^3(t,0) - \int_0^u \partial_t c \cdot \vec{n} |c_u| d\xi + \frac{1}{2}[c_t \cdot c^\perp]_0^u \\
&= \partial_t \gamma^3(t,0) - \frac{1}{2}[c_t \cdot c^\perp]_{u=0} - \int_0^1 \partial_t c \cdot \vec{n} |c_u| d\xi \\
&\quad + \int_u^1 \partial_t c \cdot \vec{n} |c_u| d\xi + \frac{1}{2}(c_t \cdot c^\perp)(t,u) \\
&= \int_u^1 \partial_t c \cdot \vec{n} |c_u| d\xi + (c_t \cdot \vec{n}) \frac{1}{2}(\vec{n} \cdot c^\perp)(t,u) + (c_t \cdot \frac{c_u}{|c_u|}) \frac{1}{2} (\frac{c_u}{|c_u|} \cdot c^\perp)(t,u) \\
&= \int_u^1 \partial_t c \cdot \vec{n} |c_u| d\xi + (c_t \cdot \vec{n}) N^3(t,u) + (c_t \cdot \frac{c_u}{|c_u|}) T^3(t,u),
\end{aligned}
$$

where we have used (3.20), (2.6) and (2.7).

So far we have totally neglected the questions about the function class and the compatibility conditions. Typically one works in the class of Hölder spaces, however, since the analysis of short and long-time existence and behaviours of the flow are outside the scope of this paper we leave out here the details and refer for instance to [22], [20] where such questions are thoroughly studied for similar problems.

3.3.1 Weak formulation used for numerics

The numerical scheme we propose hinges on a suitable weak formulation of Problem 3.7. To that end set $I = (0,1)$ and

$$
\begin{aligned}
V &:= \{(\eta_1, \eta_2, \eta_3) \,:\, \eta_\alpha \in H^{1,2}(I, \mathbb{R}^2),\ \eta_\alpha(1) = (P_\alpha^1, P_\alpha^2)^t, \alpha = 1,2,3,\ \eta_1(0) = \eta_2(0) = \eta_3(0)\}, \\
V_0 &:= \{(\eta_1, \eta_2, \eta_3) \,:\, \eta_\alpha \in H^{1,2}(I, \mathbb{R}^2),\ \eta_\alpha(1) = 0, \alpha = 1,2,3,\ \eta_1(0) = \eta_2(0) = \eta_3(0)\}.
\end{aligned}
$$

Moreover, we let

$$
W := \{(\chi_1, \chi_2, \chi_3) \,:\, \chi_\alpha \in H^{1,2}(I),\ \alpha = 1,2,3\}.
$$

Given an initial triod configuration $(c_1(0), c_2(0), c_3(0))$, find $c \in H^1(0,T;V)$, $\kappa \in L^2(0,T;W)$ and $\mu \in L^2(0,T;\mathbb{R}^3)$ such that for almost every $t \in (0,T]$ it holds that $\sum_{\alpha=1}^3 \mu_\alpha(t) = 0$ and

$$
\sum_{\alpha=1}^{3} \int_I \partial_t c_\alpha \cdot \vec{n}_\alpha \chi_\alpha |\partial_u c_\alpha| du - \sum_{\alpha=1}^{3} \int_I (\kappa_\alpha - \mu_\alpha) \chi_\alpha |\partial_u c_\alpha| du = 0 \qquad \forall\ \chi \in W, \tag{3.23a}
$$

$$\sum_{\alpha=1}^{3} \int_I \kappa_\alpha \vec{n}_\alpha \cdot \eta_\alpha |\partial_u c_\alpha| du + \sum_{\alpha=1}^{3} \int_I \partial_u c_\alpha \cdot \partial_u \eta_\alpha |\partial_u c_\alpha|^{-1} du = 0 \qquad \forall\, \eta \in V_0, \tag{3.23b}$$

$$\int_I (\kappa_1 - \mu_1)|\partial_u c_1| du = \int_I (\kappa_2 - \mu_2)|\partial_u c_2| du = \int_I (\kappa_3 - \mu_3)|\partial_u c_3| du. \tag{3.23c}$$

Upon recalling (3.22) and with the correspondence $\mu_1 = -\lambda_1$, $\mu_2 = \lambda_1 - \lambda_2$, $\mu_3 = \lambda_2$, we observe that (3.23) is the natural weak formulation of (3.18). See also [4, Remark 3.2], where a corresponding strong formulation for volume conserving mean curvature flow of a surface cluster with three surfaces and a triple junction line is given.

4 Finite element approximation

We consider a uniform partitioning of the reference domain as $\bar{I} = \bigcup_{j=1}^{J} I_j = \bigcup_{j=1}^{J} [u_{j-1}, u_j]$ with $u_j = jh$, $h = 1/J$. We then introduce the finite element spaces

$$\begin{aligned} S^h &:= \left\{ \chi \in C^0(\bar{I}) : \chi\big|_{I_j} \quad \text{is affine} \quad j = 1, \dots, J \right\}, \\ V^h &:= ([S^h]^2 \times [S^h]^2 \times [S^h]^2) \cap V, \quad V_0^h := ([S^h]^2 \times [S^h]^2 \times [S^h]^2) \cap V_0, \\ W^h &:= (S^h \times S^h \times S^h) \cap W. \end{aligned}$$

We also introduce the mass-lumped quadrature rule as

$$\int_I^h \chi \, du = \frac{h}{2} \sum_{j=1}^{J} \left[\chi(u_j^-) + \chi(u_{j-1}^+) \right],$$

for a function $\chi \in L^\infty(I)$ which is piecewise continuous with possible jumps at the nodes $\{u_j\}_{j=1}^J$, and $\chi(u_j^\pm) = \lim_{\delta \searrow 0} \chi(u_j \pm \delta)$.

We further divide the time interval uniformly by $[0, T] = \bigcup_{m=1}^{M} [t_{m-1}, t_m]$, where $t_m = m\Delta t$ and $\Delta t = T/M$ is the time step size. Let $c^m \in V^h$ be an approximation to $c(t_m)$ for $0 \le m \le M$. Throughout this section we always assume that

$$|\partial_u c_\alpha^m| > 0 \quad \text{in} \quad I, \quad \alpha = 1, 2, 3, \quad m = 0, 1, \dots, M,$$

and define the unit normal on $c_\alpha^m(I)$ via

$$\vec{n}_\alpha^m = \frac{(\partial_u c_\alpha^m)^\perp}{|\partial_u c_\alpha^m|}.$$

Our fully discrete finite element approximation of (3.23) is given as follows. Let $c^0 \in V^h$. Then, for $m \ge 0$, given $c^m \in V^h$, find $c^{m+1} = c^m + \delta c^{m+1} \in V^h$ with $\delta c^{m+1} \in V_0^h$, $\kappa^{m+1} \in W^h$ and $\mu^{m+1} \in \mathbb{R}^3$ such that $\sum_{\alpha=1}^{3} \mu_\alpha^{m+1} = 0$ and

$$\sum_{\alpha=1}^{3} \int_I^h \frac{\delta c_\alpha^{m+1}}{\Delta t} \cdot \vec{n}_\alpha^m \chi_\alpha |\partial_u c_\alpha^m| du - \sum_{\alpha=1}^{3} \int_I^h (\kappa_\alpha^{m+1} - \mu_\alpha^{m+1}) \chi_\alpha |\partial_u c_\alpha^m| du = 0 \qquad \forall\, \chi \in W^h, \tag{4.1a}$$

$$\sum_{\alpha=1}^{3} \int_I^h \kappa_\alpha^{m+1} \vec{n}_\alpha^m \cdot \eta_\alpha |\partial_u c_\alpha^m| du + \sum_{\alpha=1}^{3} \int_I \partial_u c_\alpha^{m+1} \cdot \partial_u \eta_\alpha |\partial_u c_\alpha^m|^{-1} du = 0 \qquad \forall\, \eta \in V_0^h, \tag{4.1b}$$

$$\int_I^h (\kappa_1^{m+1} - \mu_1^{m+1}) |\partial_u c_1^m| du = \int_I^h (\kappa_2^{m+1} - \mu_2^{m+1}) |\partial_u c_2^m| du = \int_I^h (\kappa_3^{m+1} - \mu_3^{m+1}) |\partial_u c_3^m| du. \tag{4.1c}$$

Observe that (4.1) is linear, and that it is the natural extension of the scheme (4.28) from [4, Remark 4.3], to the special curve network studied here.

We make the following mild assumption for the existence and uniqueness proof.

Assumption 4.1. span $\{\int_I^h \xi \vec{n}_\alpha^m |\partial_u c_\alpha^m| du : \xi \in S^h, \xi(0) = \xi(1) = 0\} \neq \{0\}$, *for* $\alpha = 1, 2, 3$.

The above assumption is very mild. A rare case when it is violated is if $J = 2$ and $c_\alpha^m(0) = c_\alpha^m(1)$. In fact, as the proof of Theorem 4.2 below will show, Assumption 4.1 can be weakened further to the span being nontrivial for just two out of the three curves. In any case, the assumption is virtually always satisfied in practice, and is in line with similar assumptions stated in the series of works [2, 1, 4, 3].

Theorem 4.2. *Let Assumptions 4.1 hold. Then there exists a unique solution to* (4.1)*. Moreover, any solution to* (4.1) *is unconditionally stable. In particular*

$$L_E(c^{m+1}) + \Delta t \sum_{\alpha=1}^{3} \int_I^h (\kappa_\alpha^{m+1} - \mu_\alpha^{m+1})^2 |\partial_u c_\alpha^m| du \leq L_E(c^m). \tag{4.2}$$

Proof. As (4.1) is a linear system with the same number of equations as unknowns, existence follows from uniqueness. It is hence sufficient to show that the homogeneous system only has the trivial solution. Let $\widehat{\delta c} \in V_0^h$, $\widehat{\kappa} \in W^h$ and $\widehat{\mu} \in \mathbb{R}^3$ be such that

$$\sum_{\alpha=1}^{3} \int_I^h \frac{\widehat{\delta c}_\alpha}{\Delta t} \cdot \vec{n}_\alpha^m \chi_\alpha |\partial_u c_\alpha^m| du - \sum_{\alpha=1}^{3} \int_I^h (\widehat{\kappa}_\alpha - \widehat{\mu}_\alpha) \chi_\alpha |\partial_u c_\alpha^m| du = 0 \qquad \forall\, \chi \in W^h, \tag{4.3a}$$

$$\sum_{\alpha=1}^{3} \int_I^h \widehat{\kappa}_\alpha \vec{n}_\alpha^m \cdot \eta_\alpha |\partial_u c_\alpha^m| du + \sum_{\alpha=1}^{3} \int_I \partial_u \widehat{\delta c}_\alpha \cdot \partial_u \eta_\alpha |\partial_u c_\alpha^m|^{-1} du = 0 \qquad \forall\, \eta \in V_0^h, \tag{4.3b}$$

$$\int_I^h (\widehat{\kappa}_1 - \widehat{\mu}_1) |\partial_u c_1^m| du = \int_I^h (\widehat{\kappa}_2 - \widehat{\mu}_2) |\partial_u c_2^m| du = \int_I^h (\widehat{\kappa}_3 - \widehat{\mu}_3) |\partial_u c_3^m| du. \tag{4.3c}$$

Choosing $\chi = \widehat{\kappa} \in W^h$ in (4.3a) and $\eta = \widehat{\delta c} \in V_0^h$ in (4.3b) yields that

$$\begin{aligned} 0 &= \sum_{\alpha=1}^{3} \int_I |\partial_u \widehat{\delta c}_\alpha|^2 |\partial_u c_\alpha^m|^{-1} du + \Delta t \sum_{\alpha=1}^{3} \int_I^h (\widehat{\kappa}_\alpha - \widehat{\mu}_\alpha) \widehat{\kappa}_\alpha |\partial_u c_\alpha^m| du \\ &= \sum_{\alpha=1}^{3} \int_I |\partial_u \widehat{\delta c}_\alpha|^2 |\partial_u c_\alpha^m|^{-1} du + \Delta t \sum_{\alpha=1}^{3} \int_I^h (\widehat{\kappa}_\alpha - \widehat{\mu}_\alpha)^2 |\partial_u c_\alpha^m| du\,, \end{aligned} \tag{4.4}$$

where we have noticed from (4.3c) that

$$\sum_{\alpha=1}^{3} \widehat{\mu}_\alpha \int_I^h (\widehat{\kappa}_\alpha - \widehat{\mu}_\alpha) |\partial_u c_\alpha^m| du = \int_I^h (\widehat{\kappa}_1 - \widehat{\mu}_1) |\partial_u c_1^m| du \sum_{\alpha=1}^{3} \widehat{\mu}_\alpha = 0. \tag{4.5}$$

It follows immediately from (4.4) that $\widehat{\delta c}$ is a constant, and hence $\widehat{\delta c} = 0$ because of the boundary conditions in V_0^h. Moreover, we have that $\widehat{\kappa}_\alpha = \widehat{\mu}_\alpha$, $\alpha = 1, 2, 3$. Combining these results with (4.3b) implies that

$$\sum_{\alpha=1}^{3} \widehat{\mu}_\alpha \int_I^h \vec{n}_\alpha^m \cdot \eta_\alpha |\partial_u c_\alpha^m| du = 0 \quad \forall\, \eta \in V_0^h. \tag{4.6}$$

Assumption 4.1 now yields that $\widehat{\mu}_\alpha = 0$, $\alpha = 1, 2, 3$. For example, for $\alpha = 1$ we choose a nonzero vector $v = \int_I^h \xi \vec{n}_1^m |\partial_u c_1^m| du$ for $\xi \in S^h$ with $\xi(0) = \xi(1) = 0$. Hence we can choose $\eta = (\widehat{\mu}_1 \xi v, 0, 0) \in V_0^h$ in (4.6) to obtain that

$$0 = \widehat{\mu}_1 \int_I^h \vec{n}_1^m \cdot (\widehat{\mu}_1 \xi v) |\partial_u c_1^m| du = (\widehat{\mu}_1)^2 v \cdot \int_I^h \vec{n}_1^m \xi |\partial_u c_1^m| du = (\widehat{\mu}_1)^2 |v|^2,$$

which implies that $\widehat{\mu}_1 = 0$. We can argue similarly to obtain $\widehat{\mu}_2 = 0$, and then $\widehat{\mu}_3 = -\widehat{\mu}_1 - \widehat{\mu}_2 = 0$. Overall we have that $(\widehat{\delta c}, \widehat{\kappa}, \widehat{\mu}) = (0, 0, 0)$. This proves the existence of a unique solution to (4.1).

In order to prove (4.2), we choose $\chi = \kappa^{m+1} \in W^h$ in (4.1a) and $\eta = \delta c^{m+1} \in V_0^h$ in (4.1b) to obtain

$$0 = \sum_{\alpha=1}^{3} \int_I \partial_u c_\alpha^{m+1} \cdot \partial_u \delta c_\alpha^{m+1} |\partial_u c_\alpha^m|^{-1} du + \Delta t \sum_{\alpha=1}^{3} \int_I^h (\kappa_\alpha^{m+1} - \mu_\alpha^{m+1}) \kappa_\alpha^{m+1} |\partial_u c_\alpha^m| du$$

$$= \sum_{\alpha=1}^{3} \int_I \partial_u c_\alpha^{m+1} \cdot \partial_u (c_\alpha^{m+1} - c_\alpha^m) |\partial_u c_\alpha^m|^{-1} du + \Delta t \sum_{\alpha=1}^{3} \int_I^h (\kappa_\alpha^{m+1} - \mu_\alpha^{m+1})^2 |\partial_u c_\alpha^m| du \,, \tag{4.7}$$

where we have noticed from (4.1c), similarly to (4.5), that

$$\sum_{\alpha=1}^{3} \mu_\alpha^{m+1} \int_I^h (\kappa_\alpha^{m+1} - \mu_\alpha^{m+1}) |\partial_u c_\alpha^m| du = \int_I^h (\kappa_1^{m+1} - \mu_1^{m+1}) |\partial_u c_1^m| du \sum_{\alpha=1}^{3} \mu_\alpha^{m+1} = 0.$$

In addition, we recall from [5, Lemma 57] that

$$\int_I \partial_u c_\alpha^{m+1} \cdot \partial_u (c_\alpha^{m+1} - c_\alpha^m) |\partial_u c_\alpha^m|^{-1} du \geq L_E(c_\alpha^{m+1}) - L_E(c_\alpha^m), \quad \alpha = 1, 2, 3. \tag{4.8}$$

Combining (4.7) and (4.8) yields the desired result (4.2). □

5 Numerical results

We implemented the scheme (4.1) within the finite element toolbox Alberta, [25], using the sparse factorization package UMFPACK, see [10], for the solution of the linear systems of equations arising at each time level. Unless otherwise stated, for the discretization parameters we always use $J = 100$ and $\Delta t = 10^{-4}$.

In order to describe the horizontal initial data, we will always state the junction point $\Sigma \in \mathbb{R}^3$ and then either state the coordinates of the fixed points $P_\alpha \in \mathbb{R}^3$, $\alpha = 1, 2, 3$, directly, or at first only specify the coordinates of their projections into the two-dimensional Euclidean plane, $\overline{P_\alpha} \in \mathbb{R}^2$, $\alpha = 1, 2, 3$, from which the missing coordinates can be computed with the help of the chosen initial planar curves via (2.2).

For the colours in our plots we follow the following convention: if the triod (or its projection) is shown at a single time $t = t_m$, then we use the colours olive, purple and gold for the curves c_1^m, c_2^m and c_3^m, respectively. If a plot shows the evolution of a triod (or its projection) at several times, then we use the colours blue, black and read for the initial data, the intermediate times and the final time, respectively.

5.1 Planar straight line initial data

In this subsection we always choose $\Sigma = (0, 0, 0)^t$ and the initial curves to be straight lines in the two-dimensional Euclidean plane. In general this means that the 120 degree angle condition at the projected triple junction $\overline{\Sigma}$ will not be satisfied at time $t = 0$.

Experiment 1: We begin with a classical Steiner configuration, that is three straight line segments that meet at the origin at 120° angles. In particular $\Sigma = (0, 0, 0)^t$, $P_1 = (-2, 0, 0)^t$, $P_2 = (1, -\sqrt{3}, 0)^t$ and $P_3 = (1, \sqrt{3}, 0)^t$. This setup is a steady state for the continuous problem, and also our finite element approximation does not change this initial data when we integrate from $t = 0$ to $t = 1$. In Figure 1 we show the initial and final discrete solution, together with a plot of the (constant) discrete energy over time.

Experiment 2: We would like to investigate what happens if we change the positions of the points P_α, $\alpha = 1, 2, 3$, in such a way, that they form a triangle with an angle larger than 120° in P_1. This is motivated by the fact that for classical curve shortening flow a singularity is expected with the triple junction Σ moving towards P_1 so that the curve c_1 eventually vanishes ([22]). We begin with a moderate setting of $P_1 = (-0.5, 0, 0)^t$, $P_2 = (1, -3, 0)^t$, $P_3 = (1, 3, 0)^t$, meaning that the angle in P_1 is 126.87°. Since we use planar straight lines for the initial curve setup, the 120° angle condition at the triple junction is violated at time $t = 0$. The evolution shown in Figure 2 demonstrates that the triod quickly relaxes to a configuration that satisfies the 120° triple junction angle condition. Eventually a steady state is approached, as can be seen from the discrete energy plots. At the final time the shortest curve has reached a length of about 0.326.

Experiment 3: In order to try to trigger an evolution towards a singularity, we make the triangle formed by P_α, $\alpha = 1, 2, 3$, even more obtuse. That is, we let $P_1 = (-0.5, 0, 0)^t$, $P_2 = (1, -9, 0)^t$, $P_3 = (1, 9, 0)^t$, meaning that the angle in P_1 is 161.06°. The evolution shown in Figure 3 indicates that now the flow does indeed encounter a singularity, as the triple junction Σ moves towards P_1, so that the curve c_1^m eventually vanishes. Note that the curve vanishing represents a singularity for our parametric formulation, and so our simulation breaks down. Observe from the combined energy plot that the remaining curves c_2^m and c_3^m are not geodesics yet.

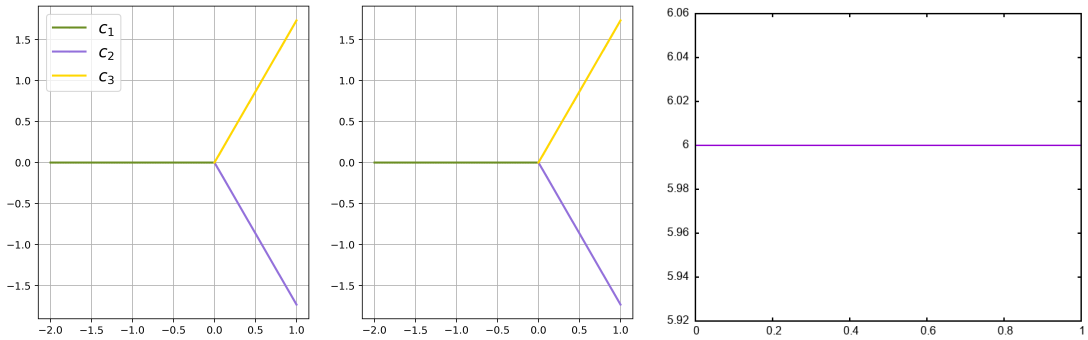

Figure 1: The triod at time $t = 0$ and at time $t = 1$. We use the colours olive, purple and gold for the curves c_1^m, c_2^m and c_3^m, respectively. On the right we show a plot of the discrete energy $L_E(c^m)$ over time.

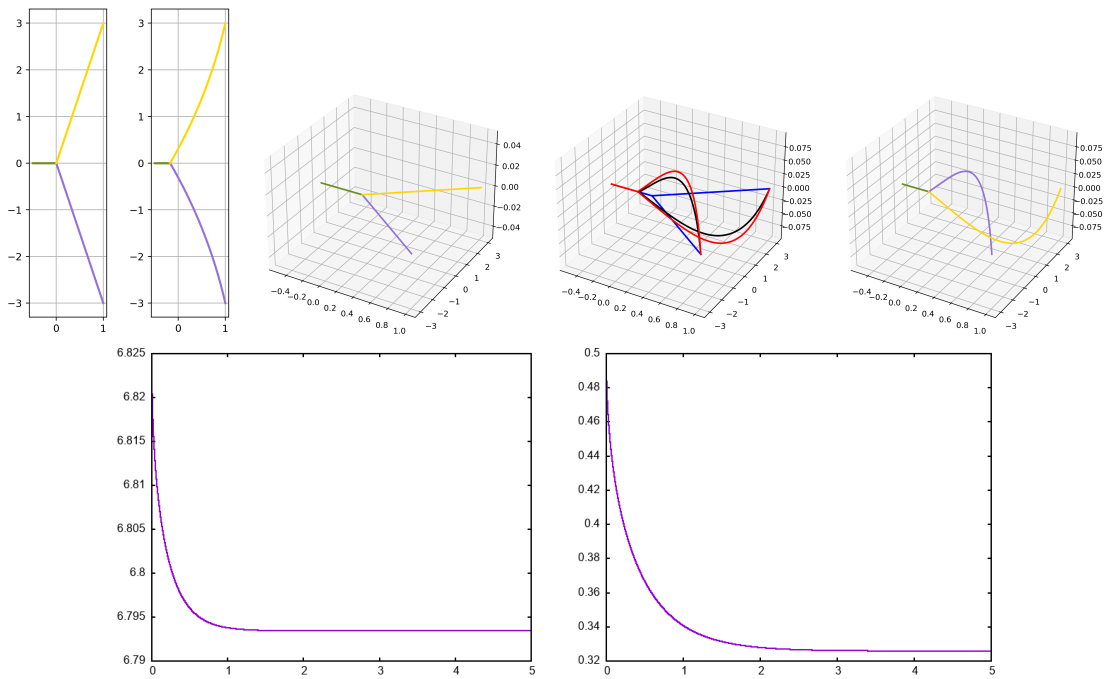

Figure 2: The projected triod at time $t = 0$ and at time $t = 5$. The triod in $\mathbb{R}^3$ is shown at time $t = 0$, at times $t = 0, 1, 5$, and at time $t = 5$. Below we show a plot of the discrete energies $L_E(c^m)$ and $L_E(c_1^m)$ over time.

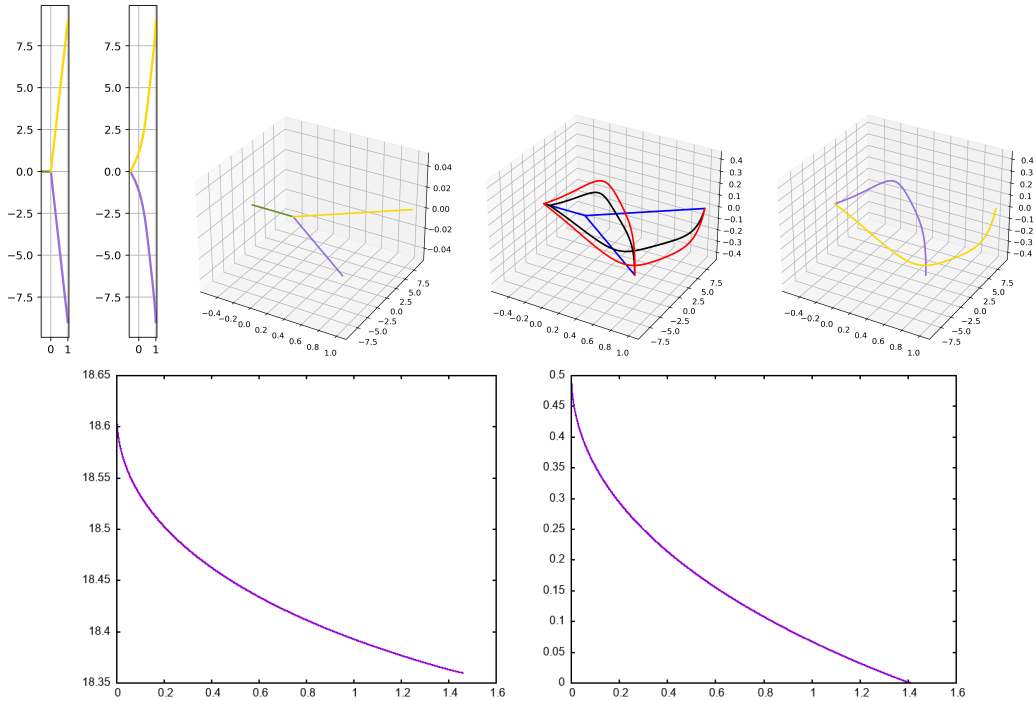

Figure 3: The projected triod at time $t = 0$ and at time $t = 1.46$. The triod in $\mathbb{R}^3$ is shown at time $t = 0$, at times $t = 0, 1, 1.46$, and at time $t = 1.46$. Below we show a plot of the discrete energies $L_E(c^m)$ and $L_E(c_1^m)$ over time.

5.2 Straight line initial data

In this subsection we choose the initial curves to be straight lines in $\mathbb{R}^3$.

Experiment 4: For this experiment we choose the location of the initial triple junction to be different from the origin. In fact, we let $\Sigma = (0, 0.1, 0)^t$ as well as $P_1 = (1, 0, -0.05)^t$, $P_2 = (0, 0, 0)^t$ and $P_3 = (\cos(\frac{2}{3}\pi), \sin(\frac{2}{3}\pi), 0.05)^t = (-0.5, \frac{1}{2}\sqrt{3}, 0.05)^t$. As a consequence, the three points $\overline{P_\alpha}$, $\alpha = 1, 2, 3$, form a triangle with an angle equal to $120°$ in $\overline{P_2}$. Once again this choice is motivated by the fact that for standard curve shortening flow in the plane the triple junction $\overline{\Sigma}$ would move towards $\overline{P_2}$, and the curve c_2 would vanish. We show the results of our scheme in Figure 4. Similarly to Figure 2, for the flow considered in this paper no singularity occurs. In fact, eventually a steady state is approached, with the shortest curve having reached a length of about 0.065.

5.3 Compatible curved initial data

In this subsection we choose the projected initial data in such a way, that the $120°$ angle condition at the triple junction is satisfied. This is achieved with the help of cubic Bézier curves, and so the initial data is in general curved. Unless otherwise stated it is $\Sigma = (0, 0, 0)^t$.

Experiment 5: We begin with an analogue of the simulation shown in Figure 2, but now with planar initial data that satisfies the $120°$ triple junction angle condition. Note that despite the projections $\overline{P_\alpha}$, $\alpha = 1, 2, 3$, being the same as before, due to the curved nature of the initial curves the points P_α, $\alpha = 1, 2, 3$, here do not lie in the two dimensional Euclidean plane. In fact, here we have $P_1 = (-0.5, 0, 0)^t$, $P_2 = (1, -3, -0.167)^t$, $P_3 = (1, 3, 0.167)^t$. We show the results from our finite element approximation in Figure 5, where we see once more that for the flow considered in this paper, no singularity arises from the chosen initial data.

Experiment 6: Correspondingly, we show an analogue of Figure 3 in Figure 6. That is, we let $P_1 = (-0.5, 0, 0)^t$, $P_2 = (1, -9, -2.74)^t$, $P_3 = (1, 9, 2.74)^t$. Similarly to before, the simulation encounters a singularity, when the shortest curve tries to vanish.

Experiment 7: Here we choose the 2d projections of P_α, $\alpha = 1, 2, 3$, to be the same, i.e. all equal to $(1, 0)^t$, with $\Sigma = (0, 0, 0)^t$. In fact, we let $P_1 = (1, 0, 0)^t$, $P_2 = (1, 0, -0.07)^t$ and $P_3 = (1, 0, 0.07)^t$. The evolution of the planar triod then converges towards a standard double bubble in the plane, see [12]. That is because the planar geodesics are given by straight lines and

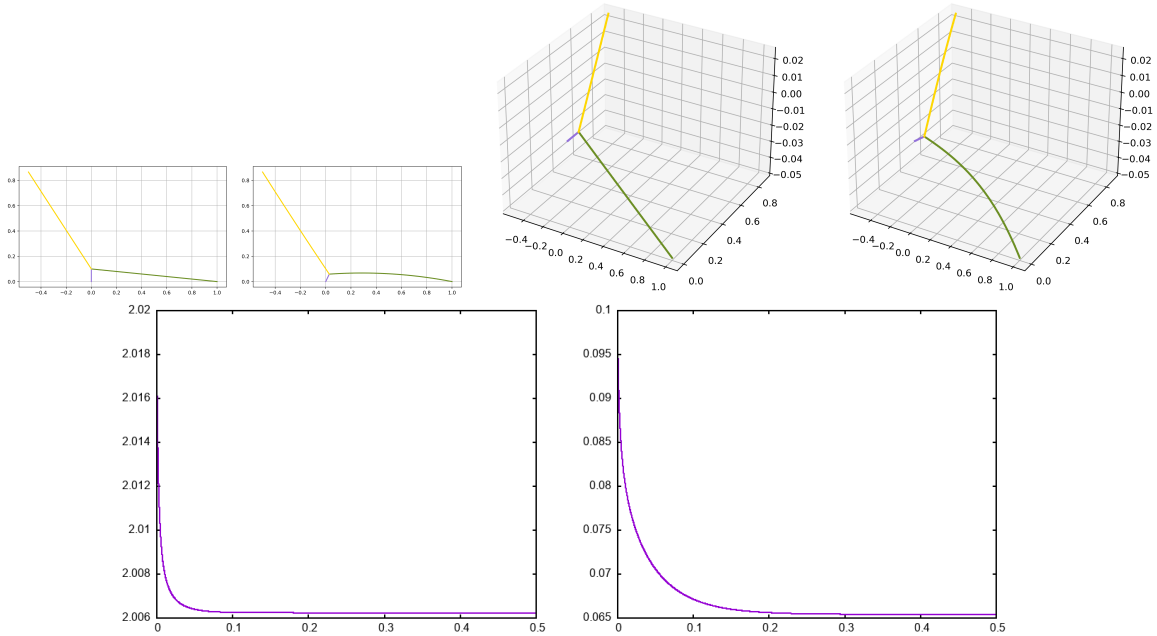

Figure 4: The (projected) triod at time $t = 0$ and at time $t = 0.5$. Below we show a plot of the discrete energies $L_E(c^m)$ and $L_E(c_2^m)$ over time.

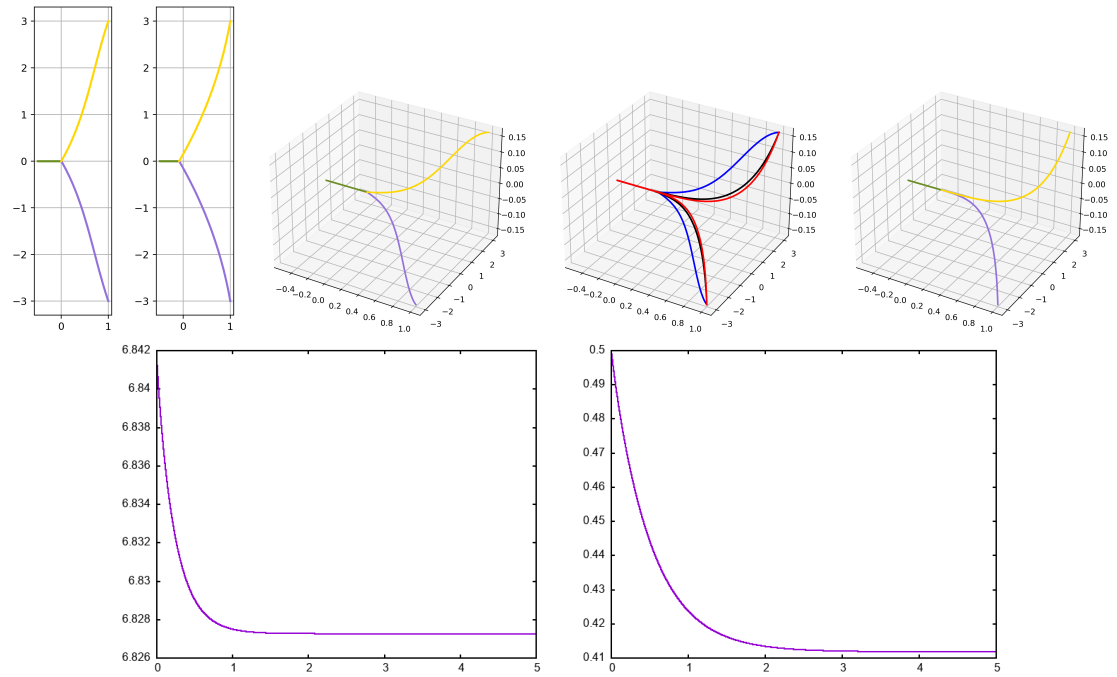

Figure 5: The projected triod at time $t = 0$ and at time $t = 5$. The triod in $\mathbb{R}^3$ is shown at time $t = 0$, at times $t = 0, 1, 5$, and at time $t = 5$. Below we show a plot of the discrete energies $L_E(c^m)$ and $L_E(c_1^m)$ over time.

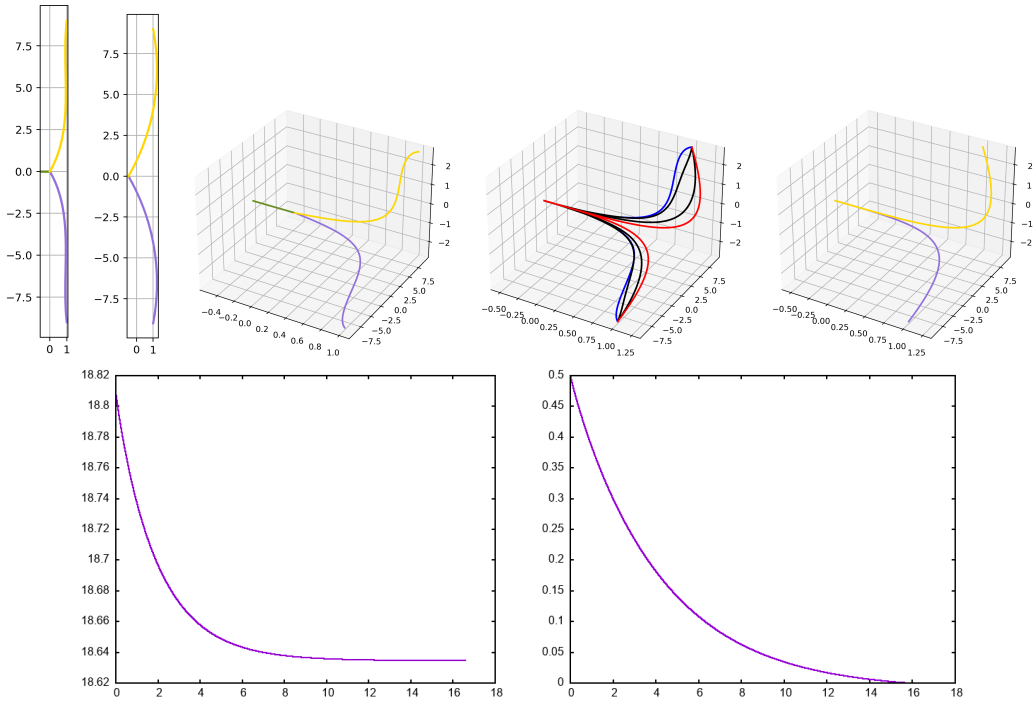

Figure 6: The projected triod at time $t = 0$ and at time $t = 16.6$. The triod in $\mathbb{R}^3$ is shown at time $t = 0$, at times $t = 0, 1, 5, 16.6$ and at time $t = 16.6$. Below we show a plot of the discrete energies $L_E(c^m)$ and $L_E(c_1^m)$ over time.

circle segments, and as they meet at 120° at $\overline{\Sigma}$, due to symmetry the same applies to the fixed planar triple junction point $(1, 0)^t$. We show the results in Figure 7. In a near repeat of the previous simulation we shift the planar initial data by one unit to the left. That is, $\Sigma = (-1, 0, 0)^t$ and $\overline{P_\alpha} = (0, 0)^t$, $\alpha = 1, 2, 3$. In fact, we have $P_1 = (0, 0, 0)^t$, $P_2 = (0, 0, -0.07)^t$ and $P_3 = (0, 0, 0.07)^t$. Since the projections will evolve exactly as shown in Figure 7, we only display the 3d curves for this experiment in Figure 8.

Experiment 8: In this experiment we choose the initial position of Σ to be $(-1, 0, 0)^t$ and let $\overline{P_\alpha} = (0, 0)^t$, $\alpha = 1, 2, 3$. In order to break the symmetry between the planar regions enclosed by c_1^0 and c_2^0, and by c_1^0 and c_3^0, we choose c_2^0 much longer than c_3^0. As a result, the planar triod now evolves towards a standard double bubble with non-equal enclosed areas. We show the results from our numerical method in Figure 9. Notice that the choice of planar initial data means that $P_1 = (0, 0, 0)^t$, $P_2 = (0, 0, -0.13)^t$ and $P_3 = (0, 0, 0.02)^t$.

Experiment 9: An even bigger imbalance between the two enclosed areas is shown in Figure 10. This time we let $\Sigma = (-1, 0, 0)^t$ and $\overline{P_\alpha} = (0, 0)^t$, $\alpha = 1, 2, 3$. Observe that the initial data is such that one of the projected curves has a self-intersection. Moreover, it holds that $P_1 = (0, 0, 0)^t$, $P_2 = (0, 0, 1.95)^t$ and $P_3 = (0, 0, 0.02)^t$.

Experiment 10: By increasing the relative lengths of the second and third curves, we manage to create an initial data from which a singularity seems to arise. That is, we let $P_1 = (0, 0, 0)^t$, $P_2 = (0, 0, 1.95)^t$, $P_3 = (0, 0, -1.04)^t$ and $\Sigma = (-1, 0, 0)^t$. In fact, for the evolution shown in Figure 11 we observe that eventually the shortest curve vanishes, because the (projected) triple junction has moved to the origin. Once again we observe that the planar initial data features self-intersections. Moreover, at the time our numerical breaks down due to the singularity, the remaining two curves do not represent geodesics. This can be seen from the negative slope of the graph of the discrete energy $L_E(c^m)$ at the final time.

Experiment 11: Another simulation with a planar setup very similar to the previous experiment is shown in Figure 12. The positions of $\Sigma = (-1, 0, 0)^t$ and $\overline{P_\alpha} = (0, 0)^t$, $\alpha = 1, 2, 3$, are as before. But this time the area enclosed by the curves c_1 and c_2 is significantly larger than the area enclosed by c_1 and c_3. In fact, we now have that $P_1 = (0, 0, 0)^t$, $P_2 = (0, 0, 1.95)^t$ and $P_3 = (0, 0, -0.39)^t$. As a consequence, the observed evolution is very different to the previous experiment. In particular, we do not observe any singularity this time. In fact, the planar evolution

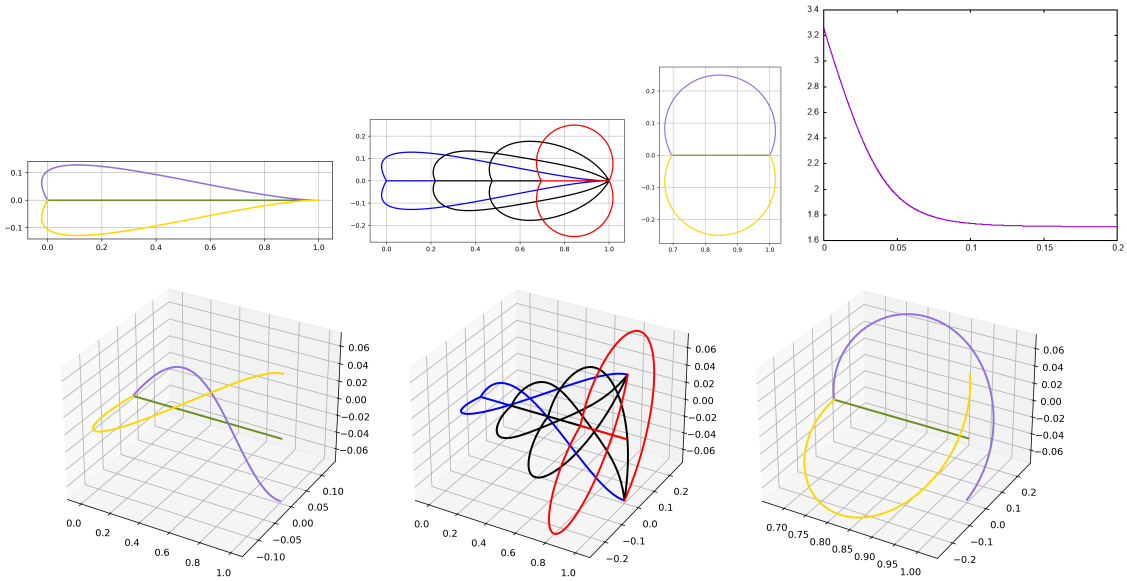

Figure 7: The (projected) triod at time $t = 0$, at times $t = 0, 0.02, 0.05, 0.2$ and at time $t = 0.2$. At the top right we show a plot of the discrete energy $L_E(c^m)$ over time.

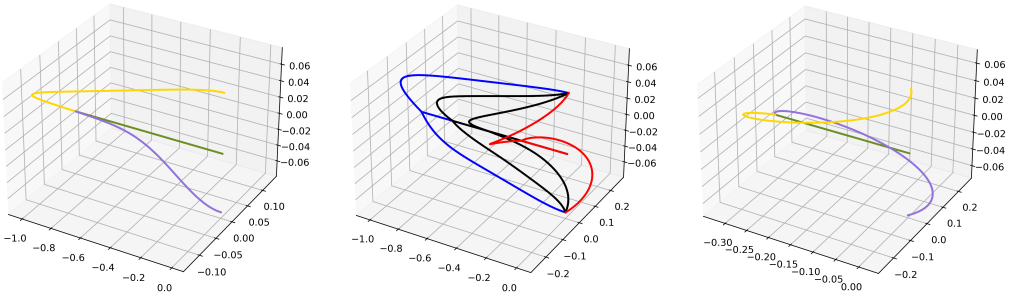

Figure 8: The triod at time $t = 0$, at times $t = 0, 0.02, 0.05, 0.2$ and at time $t = 0.2$.

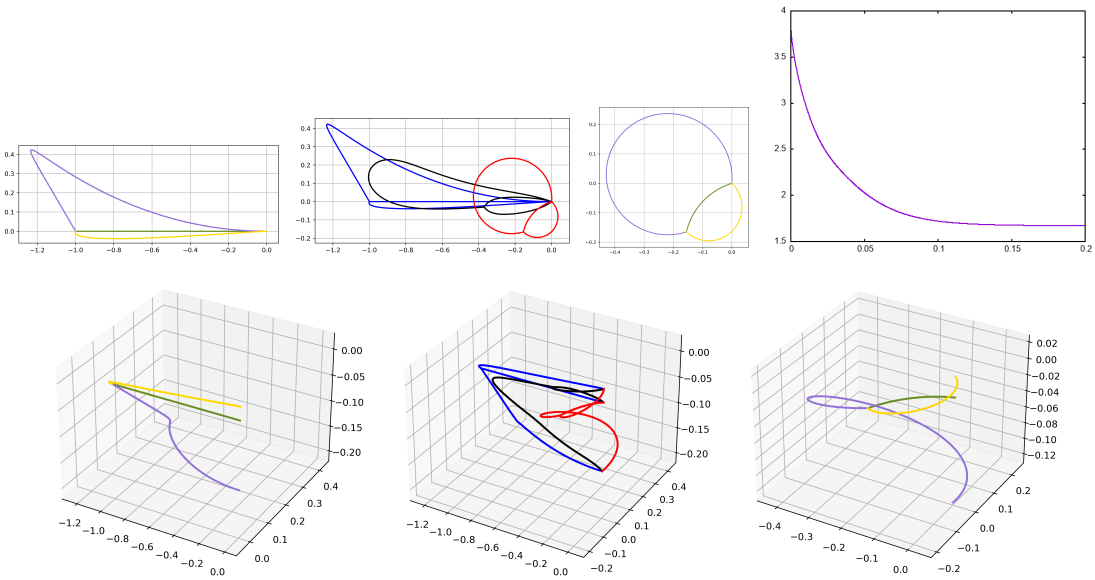

Figure 9: The (projected) triod at time $t = 0$, at times $t = 0, 0.02, 0.2$ and at time $t = 0.2$. At the top right we show a plot of the discrete energy $L_E(c^m)$ over time.

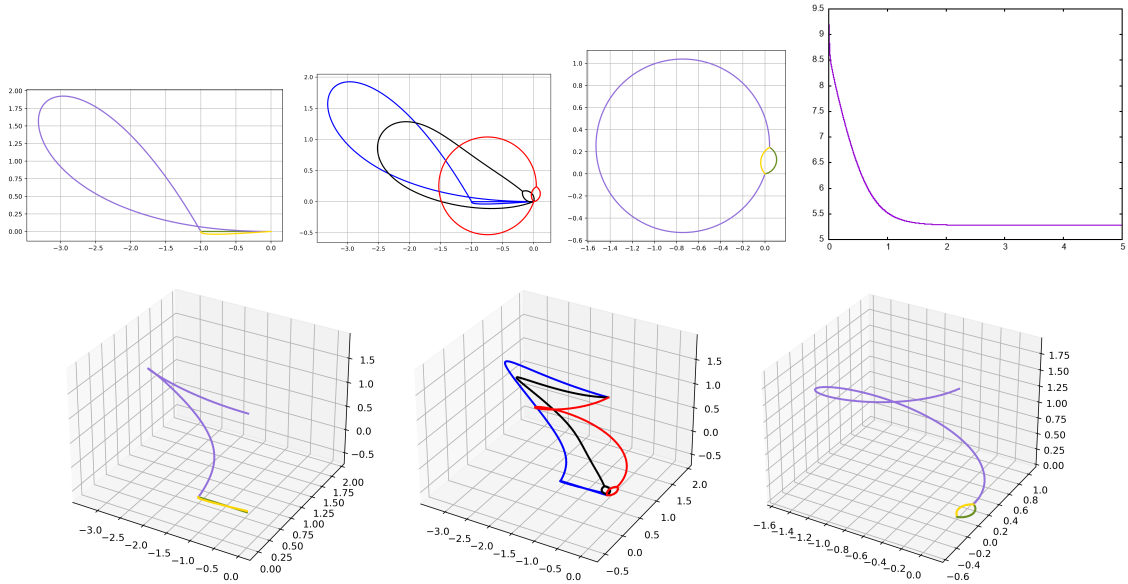

Figure 10: The (projected) triod at time $t = 0$, at times $t = 0, 0.5, 5$ and at time $t = 20$. At the top right we show a plot of the discrete energy $L_E(c^m)$ over time.

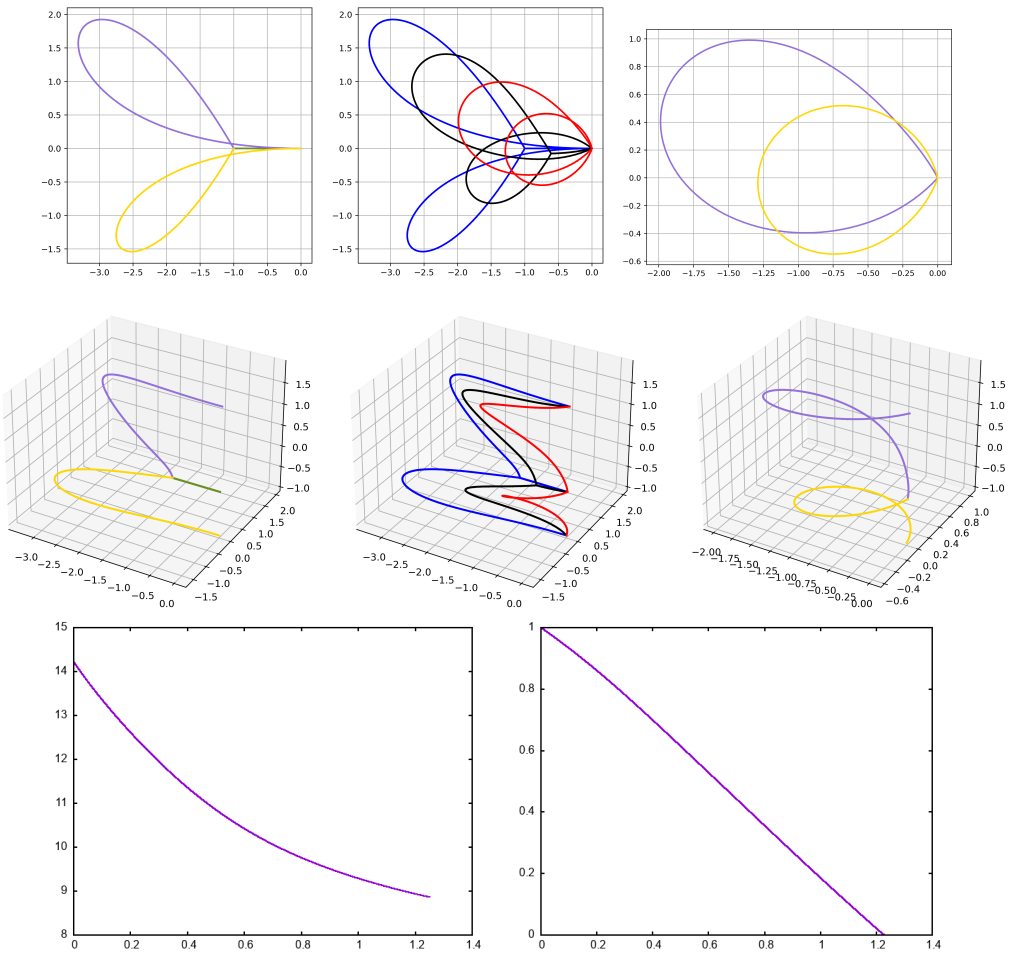

Figure 11: The (projected) triod at time $t = 0$, at times $t = 0, 0.5, 1.2$ and at time $t = 1.2$. Below we show a plot of the discrete energies $L_E(c^m)$ and $L_E(c_1^m)$ over time.

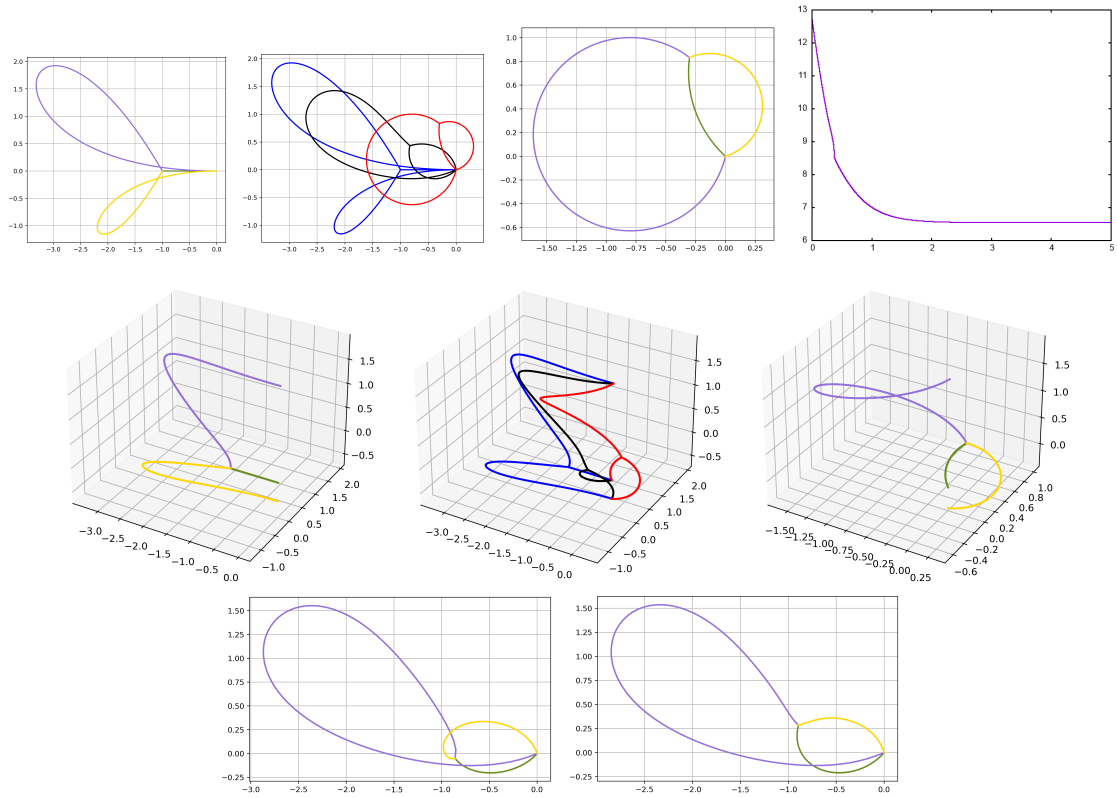

Figure 12: The (projected) triod at time $t = 0$, at times $t = 0, 0.5, 5$ and at time $t = 5$. At the top right we show a plot of the discrete energy $L_E(c^m)$ over time. In the bottom row we show the projected triod at time $t = 0.36$ and at time $t = 0.38$.

appears to approach a non-equal area standard double bubble. However, we notice a very rapid decrease in energy at around time $t = 0.37$, followed by a more moderate decrease in energy. To visualize what is causing this behaviour, we also show the projected triod shortly before and after this time at the bottom of Figure 12. What we see is that the position of the triple junction $\overline{\Sigma}$ relative to the enclosed regions changes, which we conjecture is behind the change in the speed of the energy decrease.

Experiment 12: For the initial setup we let $\Sigma = (0,0,0)^t$, as well as $\overline{P_1} = (-1,0)^t$ and $\overline{P_\alpha} = (1,0)^t$, $\alpha = 2,3$. The initial curves imply that $P_1 = (-1,0,0)^t$, $P_2 = (1,0,0.07)^t$ and $P_3 = (1,0,-0.07)^t$. In Figure 13 we observe that the planar triod evolves towards a lens steady state, as it is known from simulations for grain boundary motions or multiphase fluids. See e.g. [3, Fig. 5] and [14, Fig. 13].

5.4 Incompatible curved initial data

In this subsection we once again choose initial data for which the 120 degree angle condition at the planar triple junction is not satisfied. The initial curves will in general be curved.

Experiment 13: We choose $\Sigma = (0,0,0)^t$ and let $P_1 = (0,0,-\pi)^t$, $P_2 = (1,-\sqrt{3},0)^t$, $P_3 = (1,\sqrt{3},0)^t$. As a consequence, the 2d projections of Σ and P_1 are both equal to the origin. We display the evolution in Figure 14, where we notice that the projected triple junction $\overline{\Sigma}$ moves away from the origin and that the projected triod eventually reaches a steady state made up of three circle segments.

Experiment 14: We let $\Sigma = (0.5,-0.5,0)^t$ and $P_1 = (1,0,0)^t$, $P_2 = (0,0,0)^t$, $P_3 = (0,0,-2)^t$, and compute the initial horizontal curves connecting Σ with P_α, $\alpha = 1,2,3$, with the help of (A.2) from Example A.1, where we use the parameter $b = 1$ for each curve. The ensuing evolution is shown in Figure 15. It can be seen that the triple junction moves towards P_1, leading to a singularity when the curve c_1^m vanishes.

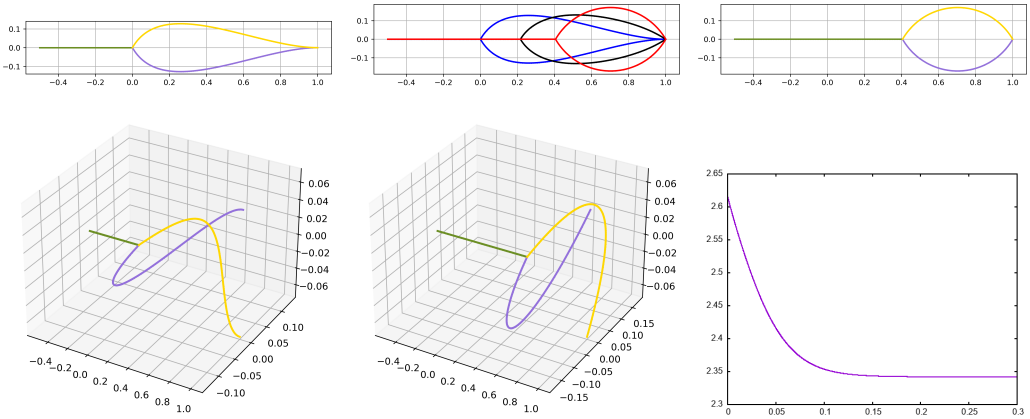

Figure 13: The projected triod at time $t = 0$, at times $t = 0, 0.05, 0.3$ and at time $t = 0.3$. Below we show the triod in $\mathbb{R}^3$ at time $t = 0$ and at time $t = 0.3$, as well as a plot of the discrete energy $L_E(c^m)$ over time.

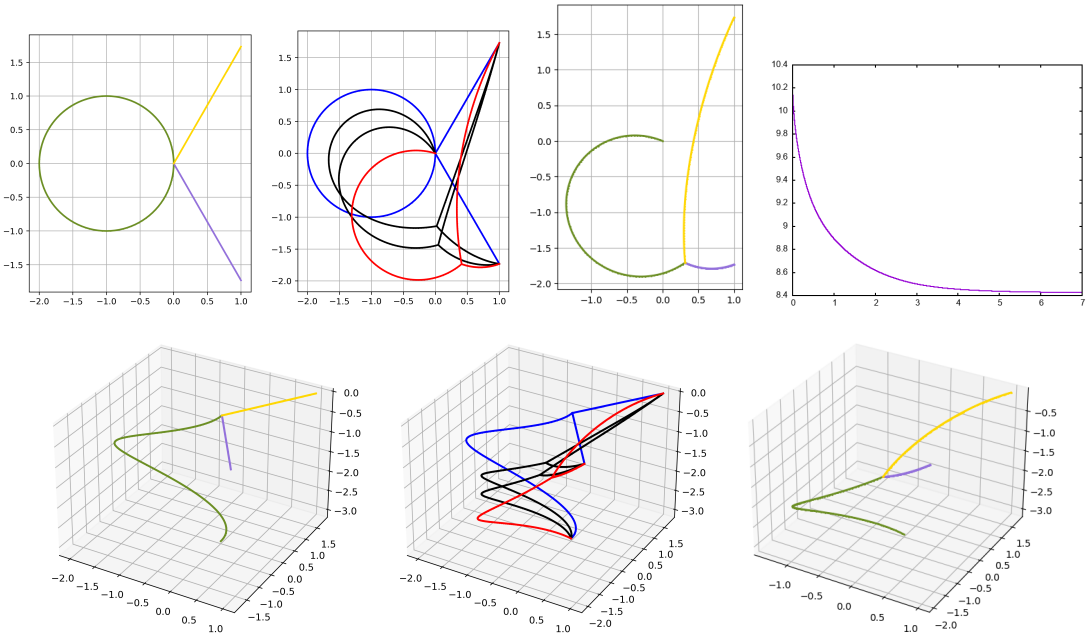

Figure 14: The (projected) triod at time $t = 0$, at times $t = 0, 1, 2, 7$ and at time $t = 7$. At the top right we show a plot of the discrete energy $L_E(c^m)$ over time.

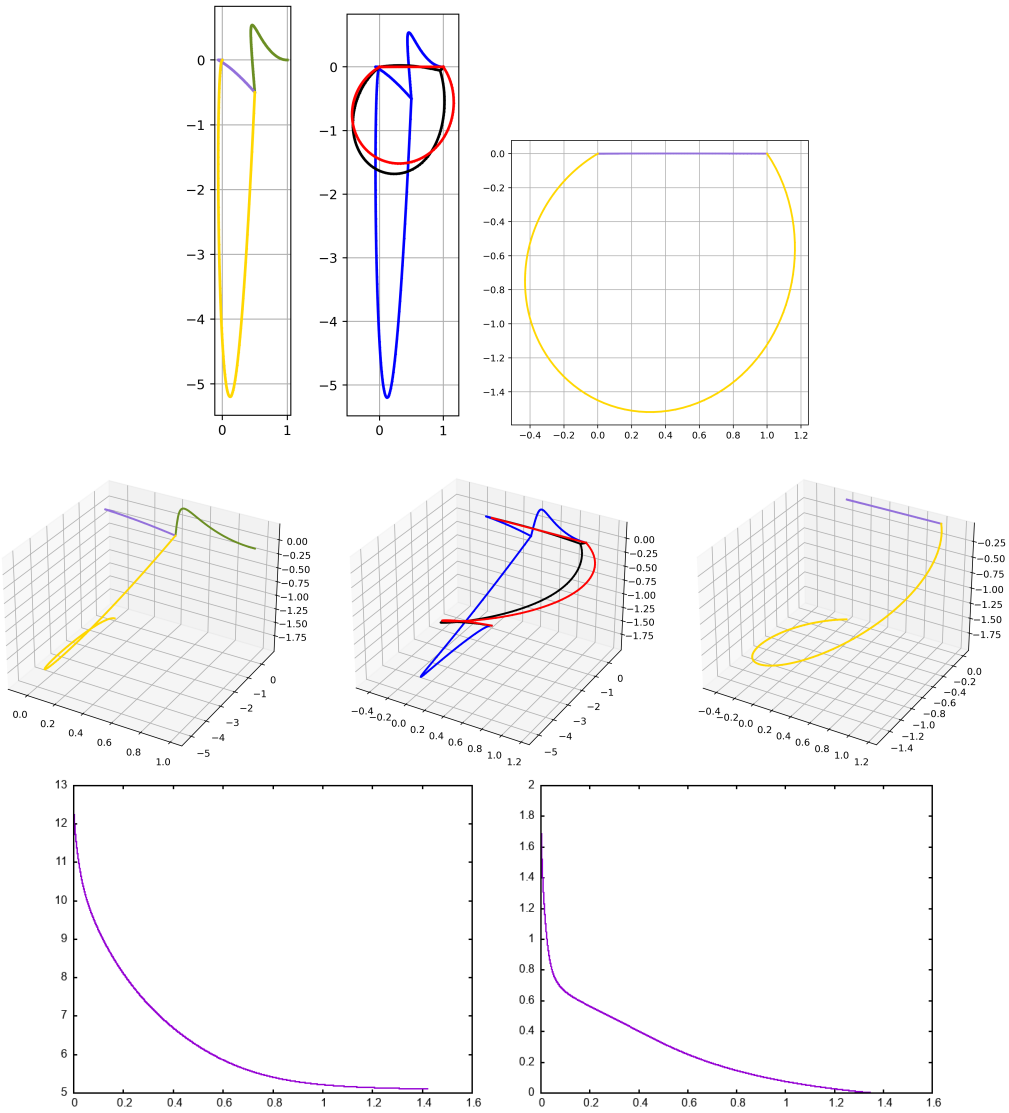

Figure 15: The (projected) triod at time $t = 0$, at times $t = 0, 1, 1.42$ and at time $t = 1.42$. Below we show a plot of the discrete energies $L_E(c^m)$ and $L_E(c_1^m)$ over time.

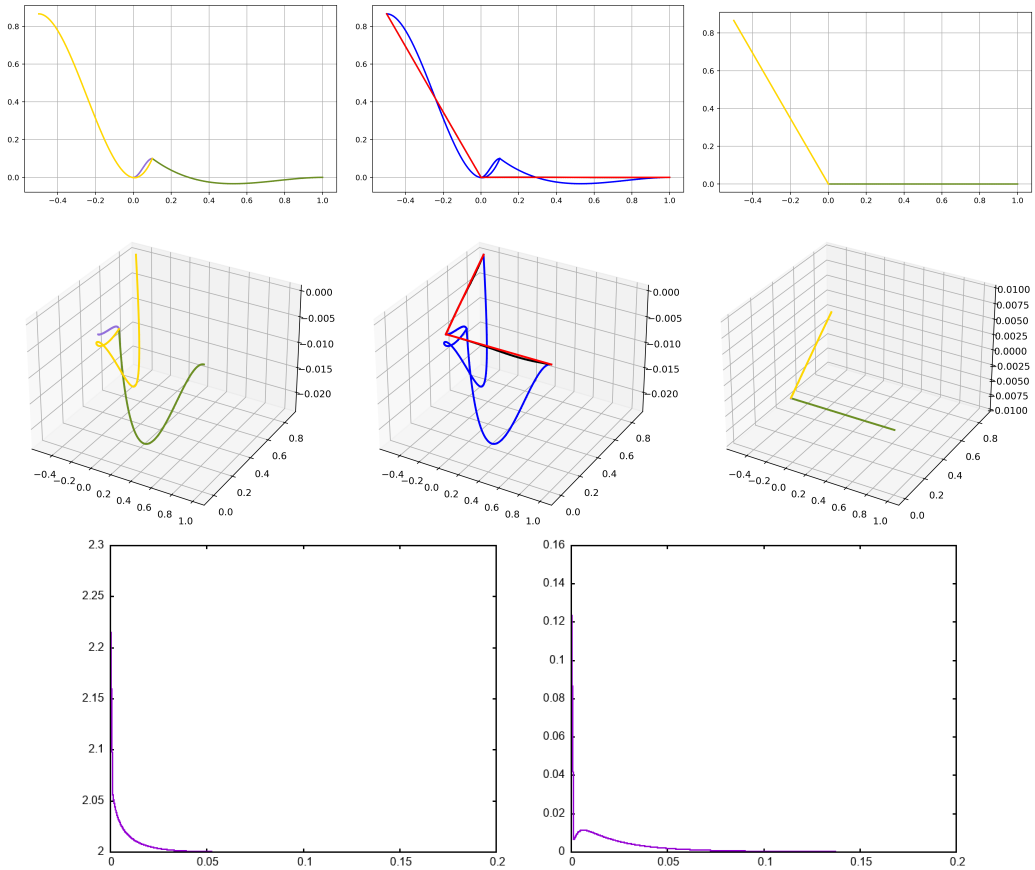

Figure 16: The (projected) triod at time $t = 0$, at times $t = 0, 0.1, 0.2$ and at time $t = 0.2$. Below we show a plot of the discrete energies $L_E(c^m)$ and $L_E(c_2^m)$ over time.

Experiment 15: We let $\Sigma = (0.1, 0.1, 0)^t$ and $P_1 = (1, 0, 0)^t$, $P_2 = (0, 0, 0)^t$, $P_3 = (\cos(\frac{2}{3}\pi), \sin(\frac{2}{3}\pi), 0)^t = (-0.5, \frac{1}{2}\sqrt{3}, 0)^t$, and once again compute the initial horizontal curves connecting Σ with P_α, $\alpha = 1, 2, 3$, with the help of (A.2), where this time we always choose $b = 0$. Observe that the points P_α form a triangle with an angle of 120 degrees in P_2. The evolution is shown in Figure 16. We observe that the projected triple junction $\overline{\Sigma}$ moves towards the origin, meaning that the curve c_2^m vanishes.

A Supporting materials

For numerical simulations it is advantageous to be able to construct horizontal curves between given points in $\mathbb{R}^3$. Following [7, Lemma 1.13] (or by direct computation) we give the following example.

Example A.1. *Let $\gamma : [0, 1] \to \mathbb{R}^3$, $\gamma = \gamma(u)$, be given through*

$$\gamma(u) = \begin{pmatrix} au + bu^2 \\ \alpha u^2 + \beta u^3 \\ \alpha a \frac{u^3}{6} + a\beta \frac{u^4}{4} + b\beta \frac{u^5}{10} \end{pmatrix}.$$

The curve γ is horizontal and passes through the origin. Let $M = (M^1, M^2, M^3)^t \in \mathbb{R}^3$. Choosing

$$\alpha = M^2 - \beta, \qquad a = M^1 - b, \qquad \beta = \frac{60M^3 - 10M^1M^2 + 10bM^2}{5M^1 + b} \tag{A.1}$$

we obtain a one-parameter family of horizontal curves (depending on b) such that $\gamma(0) = 0$ and $\gamma(1) = M$.

Let now $P, Q \in \mathbb{R}^3$ be given. Using left translation we obtain that the curves (depending on b)

$$\hat{\gamma}(u) := \tau_P(\gamma(u)) = \begin{pmatrix} P^1 + (au + bu^2) \\ P^2 + (\alpha u^2 + \beta u^3) \\ P^3 + (\alpha a \frac{u^3}{6} + a\beta \frac{u^4}{4} + b\beta \frac{u^5}{10}) + \frac{1}{2}P^1(\alpha u^2 + \beta u^3) - \frac{1}{2}P^2(au + bu^2) \end{pmatrix} \tag{A.2}$$

are horizontal curves such that $\hat{\gamma}(0) = P$ and $\hat{\gamma}(1) = Q$, provided we set

$$M^1 := Q^1 - P^1, \quad M^2 := Q^2 - P^2, \quad M^3 := Q^3 - P^3 - \frac{1}{2}(P^1(Q^2 - P^2) - P^2(Q^1 - P^1))$$

in (A.1).

Remark A.2 (Solutions of the Euler–Lagrange equations (2.14))**.** *To derive an explicit solution for curves γ satisfying* (2.14)*, we distinguish between two possible cases. In the following we let c always denote the projection of γ.*

First case: if $\lambda = 0$, i.e. $k(u) = 0$ in $[0, 1]$, then c is a straight line connecting $(P^1, P^2)^t$ and $(Q^1, Q^2)^t$, that is

$$\begin{pmatrix} \gamma^1(u) \\ \gamma^2(u) \end{pmatrix} = \begin{pmatrix} P^1 \\ P^2 \end{pmatrix} + u \begin{pmatrix} Q^1 - P^1 \\ Q^2 - P^2 \end{pmatrix}, \qquad u \in [0, 1].$$

From (2.2) *a straightforward calculation yields*

$$\gamma^3(u) = P^3 + u\left(-\frac{1}{2}P^2Q^1 + \frac{1}{2}P^1Q^2\right) \qquad u \in [0, 1],$$

and Q^3 must satisfy the equation $Q^3 = P^3 - \frac{1}{2}P^2Q^1 + \frac{1}{2}P^1Q^2$. We can write the straight line also as the horizontal curve

$$\gamma(u) = P + u(Q^1 - P^1)X_1(P) + u(Q^2 - P^2)X_2(P)$$

in the horizontal plane through P. Observe that if P is the origin (which we can always attain after an appropriate left translation, recall Lemma 2.4), then the line lies in the (x, y)-plane.

Second case: if $\lambda \neq 0$ then the Euler–Lagrange equations yield

$$\frac{1}{|c'|}\left(\frac{1}{|c'|}\gamma^1_u\right)_u = \lambda \frac{\gamma^2_u}{|c'|} \quad \text{in } (0, 1),$$
$$\frac{1}{|c'|}\left(\frac{1}{|c'|}\gamma^2_u\right)_u = -\lambda \frac{\gamma^1_u}{|c'|} \quad \text{in } (0, 1).$$

Reparametrizing c by arc length (i.e. $|c'(s)| = 1$, $ds = |c'(u)|du$), the above system reads

$$\gamma^1_{ss} = \lambda\gamma^2_s, \qquad \gamma^2_{ss} = -\lambda\gamma^1_s \qquad \text{for } s \in (0, L_E(c)),$$

i.e.

$$c_{ss} = \lambda J c_s, \qquad \text{with } J = \begin{pmatrix} 0 & 1 \\ -1 & 0 \end{pmatrix},$$

with solution $c_s(s) = e^{\lambda J s}c_s(0) = \begin{pmatrix} \cos(\lambda s) & \sin(\lambda s) \\ -\sin(\lambda s) & \cos(\lambda s) \end{pmatrix} c_s(0)$ (cf. [7, Lemma 1.16]). Integration gives

$$c(s) = c(0) + \int_0^s e^{\lambda J \xi}c_s(0)d\xi = c(0) + \left[\frac{1}{\lambda}J^{-1}e^{\lambda J\xi}c_s(0)\right]_0^s = c(0) - \frac{1}{\lambda}J^{-1}c_s(0) + \frac{1}{\lambda}J^{-1}e^{\lambda J s}c_s(0).$$

Therefore a general solution is of type

$$c(s) = A + \frac{1}{\lambda}\begin{pmatrix} 0 & -1 \\ 1 & 0 \end{pmatrix}\begin{pmatrix} \cos(\lambda s) & \sin(\lambda s) \\ -\sin(\lambda s) & \cos(\lambda s) \end{pmatrix} B = A + \frac{1}{\lambda}\begin{pmatrix} \sin(\lambda s) & -\cos(\lambda s) \\ \cos(\lambda s) & \sin(\lambda s) \end{pmatrix} B,$$

for vectors $A, B \in \mathbb{R}^2$, with $B = c_s(0)$ and $A = c(0) - \frac{1}{\lambda}J^{-1}c_s(0)$. In particular, we see that the projected curve c is an arc of a circle of radius $|B|/|\lambda| = \frac{1}{|\lambda|}$ (since $|B| = |c_s(0)| = 1$ due to the arc length parametrization). Writing

$$c_s(0) = B = (\cos(\alpha_0), \sin(\alpha_0))^t$$

for some $\alpha_0 \in [0, 2\pi)$, we obtain

$$c(s) = A + \frac{1}{\lambda}\begin{pmatrix} \sin(\lambda s) & -\cos(\lambda s) \\ \cos(\lambda s) & \sin(\lambda s) \end{pmatrix}\begin{pmatrix} \cos(\alpha_0) \\ \sin(\alpha_0) \end{pmatrix} = A + \frac{1}{\lambda}\begin{pmatrix} \sin(\lambda s - \alpha_0) \\ \cos(\lambda s - \alpha_0) \end{pmatrix}. \tag{A.3}$$

The constants A, B are determined through the equations

$$\begin{pmatrix} P^1 \\ P^2 \end{pmatrix} = c(0) = A + \frac{1}{\lambda}\begin{pmatrix} 0 & -1 \\ 1 & 0 \end{pmatrix} B$$

and, with $s_f := L_E(c) = L(\gamma)$,

$$\begin{pmatrix} Q^1 \\ Q^2 \end{pmatrix} = c(s_f) = A + \frac{1}{\lambda}\begin{pmatrix} \sin(\lambda s_f) & -\cos(\lambda s_f) \\ \cos(\lambda s_f) & \sin(\lambda s_f) \end{pmatrix} B.$$

This gives for $\lambda s_f \in (0, 2\pi) + 2\pi\mathbb{Z}$:

$$\begin{aligned} B &= \frac{\lambda}{\sin^2(\lambda s_f) + (1-\cos(\lambda s_f))^2}\begin{pmatrix} \sin(\lambda s_f) & \cos(\lambda s_f) - 1 \\ 1 - \cos(\lambda s_f) & \sin(\lambda s_f) \end{pmatrix}\begin{pmatrix} Q^1 - P^1 \\ Q^2 - P^2 \end{pmatrix} \\ &= \frac{\lambda}{2(1-\cos(\lambda s_f))}\begin{pmatrix} \sin(\lambda s_f) & \cos(\lambda s_f) - 1 \\ 1 - \cos(\lambda s_f) & \sin(\lambda s_f) \end{pmatrix}\begin{pmatrix} Q^1 - P^1 \\ Q^2 - P^2 \end{pmatrix}, \end{aligned} \tag{A.4}$$

$$A = \begin{pmatrix} P^1 \\ P^2 \end{pmatrix} - \frac{1}{\lambda}\begin{pmatrix} 0 & -1 \\ 1 & 0 \end{pmatrix} B. \tag{A.5}$$

We deduce in particular that $(P^1, P^2) \neq (Q^1, Q^2)$. After computing the expressions (A.4), (A.5), *we obtain the curve c by expression* (A.3). *The third component of the horizontal lift of c starting at P is finally computed via* (2.2), *and hence Q^3 must satisfy*

$$\begin{aligned} Q^3 &= P^3 + \int_0^{s_f} \left(-\frac{1}{2}\gamma^2(s)\gamma_s^1(s) + \frac{1}{2}\gamma^1(s)\gamma_s^2(s) \right) ds \\ &= P^3 + \int_0^{s_f} \Big(-\frac{1}{2}A^2[B^1\cos(\lambda s) + B^2\sin(\lambda s)] + \frac{1}{2}A^1[B^2\cos(\lambda s) - B^1\sin(\lambda s)] - \frac{|B|^2}{2\lambda} \Big) ds. \end{aligned}$$

In particular if $P = 0$ (which we can always attain after appropriate left translation) then $A^1 = \frac{1}{\lambda}B^2$, $A^2 = -\frac{1}{\lambda}B^1$ and

$$\gamma^3(s) = -\frac{1}{2\lambda}s + \frac{1}{2\lambda^2}\sin(\lambda s) = \frac{\sin(\lambda s) - \lambda s}{2\lambda^2} \qquad \text{for } s \in [0, s_f], \tag{A.6}$$

so that

$$Q^3 = \frac{\sin(\lambda s_f) - \lambda s_f}{2\lambda^2}. \tag{A.7}$$

If $\lambda s_f = 2\pi k$, for some $k \in \mathbb{Z}$, then $(P^1, P^2) = (Q^1, Q^2) = c(0)$, i.e. the projected curve c is a (k-multiply covered) circle, whereby we have freedom in choosing the vector $B = c_s(0) = (\cos(\alpha_0), \sin(\alpha_0))^t$ for $\alpha_0 \in [0, 2\pi)$. For this one-parameter family of solutions we obtain by (2.2) *and* (A.3) *that*

$$Q^3 = P^3 + \int_0^{\lambda s_f} -\frac{1}{2}\gamma^2(s)\gamma_s^1(s) + \frac{1}{2}\gamma^1(s)\gamma_s^2(s)ds = P^3 - (2\pi k)\frac{|B|^2}{2\lambda^2}.$$

In particular

$$|Q_3 - P_3| = \frac{(2\pi|k|)}{2\lambda^2} = \frac{\pi|k|}{\lambda^2}.$$

Note that unlike the Euclidean setting, we have here a one-parameter family of solution curves having all the same length.

B Horizontal curve shortening flow

Although Remark A.2 (see also [7, §1.6] for further information) fully describes horizontal curves of minimal length, an alternative way to obtain the critical points (2.14), is to let a given horizontal curve flow into a critical configuration. This approach is interesting in its own right. In the following we provide an informal definition of such a flow and call it horizontal curve shortening flow.

Assumption B.1. *Let $P \neq Q$ be two given points in $\mathbb{R}^3$ and let $\gamma_0 : [0,1] \to \mathbb{R}^3$ be a regular smooth horizontal curve connecting P and Q.*

Taking into consideration Remark 2.12, (2.8), and Lemma 2.10, it is natural to consider the following flow, which we call *horizontal curve shortening flow*:

Problem B.2. *Let Assumption B.1 hold. Find $\gamma : [0,T) \times [0,1] \to \mathbb{R}^3$, $\gamma = \gamma(t,u)$, which satisfies $\gamma(0,\cdot) = \gamma_0$, and*

$$\gamma_t(t,u) = \vec{k}_g(t,u) + \lambda(t)N(t,u) - \Big(\int_0^u (k(t,\xi) + \lambda(t))|\gamma_u(t,\xi)|_g d\xi\Big) X_3(\gamma(t,u)) \qquad \text{for all } (t,u) \in (0,T) \times (0,1),$$

$$\gamma(t,0) = P \quad \text{for all } t \in (0,T),$$
$$\gamma(t,1) = Q \quad \text{for all } t \in (0,T),$$

where

$$\lambda(t) = -\frac{\int_0^1 k(t,u)|\gamma_u(t,u)|_g du}{L(\gamma(t))}.$$

Lemma B.3. *If $\gamma : [0,T) \times [0,1] \to \mathbb{R}^3$ is a solution to Problem B.2, then the length $L(\gamma(t))$ of the horizontal curve $\gamma(t)$ decreases along the flow.*

Proof. A direct computation gives

$$\begin{aligned}
\frac{d}{dt}L(\gamma(t)) &= \frac{d}{dt}\int_0^1 \sqrt{(\gamma_u^1)^2 + (\gamma_u^2)^2} du \\
&= -\int_0^1 \frac{1}{|\gamma_u|_g}\left(\frac{1}{|\gamma_u|_g}\begin{pmatrix}\gamma_u^1\\ \gamma_u^2\end{pmatrix}\right)_u \cdot \begin{pmatrix}\gamma_t^1\\ \gamma_t^2\end{pmatrix} |\gamma_u|_g du + \left[\frac{1}{|\gamma_u|_g}\begin{pmatrix}\gamma_u^1\\ \gamma_u^2\end{pmatrix} \cdot \begin{pmatrix}\gamma_t^1\\ \gamma_t^2\end{pmatrix}\right]_0^1 \\
&= -\int_0^1 k(k+\lambda)|\gamma_u|_g du = -\int_0^1 k^2|\gamma_u|_g du - \lambda\int_0^1 k|\gamma_u|_g du \leq 0,
\end{aligned}$$

where we have used that $\gamma_t = 0$ at the boundary, the definition of λ, and a Hölder inequality. □

Note that if γ solves the above horizontal curve shortening flow (Problem B.2), then its projected curve $c = (\gamma^1, \gamma^2)^t$ satisfies the following problem in the Euclidean setting:

Problem B.4. *Let Assumption B.1 hold. Find $c : [0,T) \times [0,1] \to \mathbb{R}^2$, $c = (\gamma^1, \gamma^2)^t$, which satisfies $\gamma^r(0,\cdot) = \gamma_0^r$ for $r = 1,2$, and*

$$\begin{aligned}
c_t(t,u) &= \vec{k}(t,u) + \lambda(t)\vec{n}(t,u) \qquad \text{for all } (t,u) \in (0,T) \times (0,1), \\
c(t,0) &= (P^1, P^2)^t \quad \text{for all } t \in (0,T), \\
c(t,1) &= (Q^1, Q^2)^t \quad \text{for all } t \in (0,T),
\end{aligned} \tag{B.1}$$

where

$$\begin{aligned}
\vec{n}(t,u) &:= \frac{1}{|c_u(t,u)|}\begin{pmatrix}-\gamma_u^2(t,u)\\ \gamma_u^1(t,u)\end{pmatrix}, \\
\lambda(t) &= -\frac{\int_0^1 k(t,u)|c_u(t,u)|du}{L_E(c(t))} = -\frac{\int_0^1 \vec{k}(t,u)\cdot\vec{n}(t,u)|c_u(t,u)|du}{L_E(c(t))}.
\end{aligned} \tag{B.2}$$

On the other hand, if $c = (\gamma^1, \gamma^2)^t$ is a solution of Problem B.4 then its horizontal lift $\gamma : [0,T) \times [0,1] \to \mathbb{R}^3$ with

$$\gamma^3(t,u) = P^3 + \int_0^u \left(-\frac{1}{2}\gamma^2(t,\xi)\gamma_u^1(t,\xi) + \frac{1}{2}\gamma^1(t,\xi)\gamma_u^2(t,\xi) \right) d\xi$$

yields (using integration by parts and the fact that $\gamma_t^1 = \gamma_t^2 = 0$ at the boundary)

$$\begin{aligned}
\gamma_t^3(t,u) &= \int_0^u \left(-\frac{1}{2}\gamma_t^2\gamma_u^1 - \frac{1}{2}\gamma^2\gamma_{tu}^1 + \frac{1}{2}\gamma_t^1\gamma_u^2 + \frac{1}{2}\gamma^1\gamma_{tu}^2 \right) d\xi \\
&= \int_0^u \left(-\gamma_t^2\gamma_u^1 + \gamma_t^1\gamma_u^2 \right) d\xi + \frac{1}{2}\gamma^1(u)\gamma_t^2(u) - \frac{1}{2}\gamma^2(u)\gamma_t^1(u) \\
&= \int_0^u \left(-\gamma_t^2\gamma_u^1 + \gamma_t^1\gamma_u^2 \right) d\xi + \frac{1}{2}\gamma^1(u)(k(t,u)+\lambda(t))\frac{\gamma_u^1}{|c_u|} - \frac{1}{2}\gamma^2(u)(k(t,u)+\lambda(t))(-\frac{\gamma_u^2}{|c_u|}) \\
&= \vec{k}_g^3(t,u) + \lambda(t)N^3(t,u) + \int_0^u -(k+\lambda)n^2n^2|c_u| + (k+\lambda)n^1(-n^1|c_u|)d\xi \\
&= \vec{k}_g^3(t,u) + \lambda(t)N^3(t,u) - \int_0^u (k+\lambda(t))|c_u|d\xi.
\end{aligned}$$

By assumption γ_0^3 fulfills the boundary conditions and has the structure given in (2.2). By Lemma 2.10 the component $\gamma^3(t,\cdot)$ maintains this structure and fulfills the boundary and initial condition. Hence we see that by taking the horizontal lift of a solution to Problem B.4, we recover a solution to Problem B.2.

Remark B.5. *(i) Note that Assumption B.1 restricts the class of initial curves for which Problem B.4 is solved (recall Remark 2.3).*

(ii) Recall that $\int_0^1 k|c_u|du = \theta(1) - \theta(0)$, where θ is the angle that the unit tangent of the planar curve c makes with the x-axis. Even if $(P^1, P^2)^t = (Q^1, Q^2)^t$, the quantity $(\theta(1) - \theta(0))$ need not be a multiple of 2π, since no angle condition is imposed at the boundary. In other words, the projected curve might be closed, in the sense that $c(0) = c(1)$, but not smooth across $c(0) = c(1)$.

Remark B.6. *As in Lemma B.3, we see that $\frac{d}{dt}L_E(c(t)) \leq 0$ for a smooth solution to Problem B.4. We give here a different way to derive the same result, as it provides further geometrical insight into the role of the Lagrange multiplier. Using that $c_t = 0$ at the boundary we infer*

$$\begin{aligned}
\frac{d}{dt}L_E(c(t)) &= \int_0^1 \frac{c_u}{|c_u|} \cdot c_{tu} du \\
&= \left[\frac{c_u}{|c_u|} \cdot c_t \right]_0^1 - \int_0^1 \vec{k} \cdot c_t |c_u| du = -\int_0^1 |c_t|^2 |c_u| du + \lambda(t) \int_0^1 \vec{n} \cdot c_t |c_u| du.
\end{aligned}$$

Note that for a smooth solution of the flow we have

$$\lambda(t) = -\frac{\int_0^1 k(t,u)|c_u|du}{L_E(c(t))} = -\frac{\int_0^1 \vec{k}(t,u) \cdot \vec{n}(t,u)|c_u|du}{L_E(c(t))} = -\frac{\int_0^1 c_t \cdot \vec{n}|c_u|du}{L_E(c(t))} + \lambda(t),$$

so that we infer (compare with Remark 2.3 for a geometric interpretation)

$$0 = \int_0^1 c_t \cdot \vec{n}|c_u|du = \frac{d}{dt}\left(\int_0^1 \frac{1}{2} \begin{pmatrix} \gamma^1(u) \\ \gamma^2(u) \end{pmatrix} \cdot \begin{pmatrix} -\gamma_u^2(u) \\ \gamma_u^1(u) \end{pmatrix} du \right) + \frac{1}{2}[c_t \cdot c^\perp]_0^1$$

and

$$\frac{d}{dt}L_E(c(t)) = -\int_0^1 |c_t|^2|c_u|du + \lambda(t)\int_0^1 \vec{n} \cdot c_t|c_u|du = -\int_0^1 |c_t|^2|c_u|du \leq 0.$$

Remark B.7. *The Euclidean evolution* (B.1), (B.2) *has been studied analytically in different settings subject to different boundary conditions: for instance for smooth closed (i.e. periodic) curves (where $\int_0^1 k|c_u|du = 2\pi m$, for $m \in \mathbb{Z}$) see [13]; for the study of the area preserving curve shortening flow with Neumann free boundary conditions outside of a convex domain in the plane see [21]. Evolution by mean curvature flow for Legendre submanifolds in a Sazaki manifold is studied in [26]. The evolution of closed curves in $\mathcal{H}$ by a flow related to Problem B.2 is investigated in [11] and [24]: there, due to objectives that differs from ours, the projected curves evolve by the standard curve shortening flow (and their initial closed curves c_0 cannot be embedded due to the horizontality condition (recall Remark 2.3)).*

References

[1] Barrett, J. W., Garcke, H., and Nürnberg, R. On the variational approximation of combined second and fourth order geometric evolution equations. *SIAM J. Sci. Comput. 29*, 3 (2007), 1006–1041.

[2] Barrett, J. W., Garcke, H., and Nürnberg, R. A parametric finite element method for fourth order geometric evolution equations. *J. Comput. Phys. 222*, 1 (2007), 441–462.

[3] Barrett, J. W., Garcke, H., and Nürnberg, R. Finite element approximation of coupled surface and grain boundary motion with applications to thermal grooving and sintering. *European J. Appl. Math. 21*, 6 (2010), 519–556.

[4] Barrett, J. W., Garcke, H., and Nürnberg, R. Parametric approximation of surface clusters driven by isotropic and anisotropic surface energies. *Interfaces Free Bound. 12*, 2 (2010), 187–234.

[5] Barrett, J. W., Garcke, H., and Nürnberg, R. Parametric finite element approximations of curvature driven interface evolutions. In *Handb. Numer. Anal.*, A. Bonito and R. H. Nochetto, Eds., vol. 21. Elsevier, Amsterdam, 2020, pp. 275–423.

[6] Buttazzo, G., Giaquinta, M., and Hildebrandt, S. *One-dimensional variational problems*, vol. 15 of *Oxford Lecture Series in Mathematics and its Applications*. The Clarendon Press, Oxford University Press, New York, 1998. An introduction.

[7] Calin, O., Chang, D.-C., and Greiner, P. *Geometric analysis on the Heisenberg group and its generalizations*, vol. 40 of *AMS/IP Studies in Advanced Mathematics*. American Mathematical Society, Providence, RI; International Press, Somerville, MA, 2007.

[8] Capogna, L., Danielli, D., Pauls, S. D., and Tyson, J. T. *An introduction to the Heisenberg group and the sub-Riemannian isoperimetric problem*, vol. 259 of *Progress in Mathematics*. Birkhäuser Verlag, Basel, 2007.

[9] Dacorogna, B. *Direct methods in the calculus of variations*, second ed., vol. 78 of *Applied Mathematical Sciences*. Springer, New York, 2008.

[10] Davis, T. A. Algorithm 832: UMFPACK V4.3—an unsymmetric-pattern multifrontal method. *ACM Trans. Math. Software 30*, 2 (2004), 196–199.

[11] Drugan, G., He, W., and Warren, M. W. Legendrian curve shortening flow in $\mathbb{R}^3$. *Comm. Anal. Geom. 26*, 4 (2018), 759–785.

[12] Foisy, J., Alfaro, M., Brock, J., Hodges, N., and Zimba, J. The standard double soap bubble in $\mathbb{R}^2$ uniquely minimizes perimeter. *Pacific J. Math. 159*, 1 (1993), 47–59.

[13] Gage, M. On an area-preserving evolution equation for plane curves. In *Nonlinear problems in geometry (Mobile, Ala., 1985)*, vol. 51 of *Contemp. Math.* Amer. Math. Soc., Providence, RI, 1986, pp. 51–62.

[14] Garcke, H., Nürnberg, R., and Zhao, Q. A variational front-tracking method for multiphase flow with triple junctions. *Math. Comp.* (2025). (to appear).

[15] Gilbert, E. N., and Pollak, H. O. Steiner minimal trees. *SIAM Journal on Applied Mathematics 16*, 1 (1968), 1–29.

[16] Hildebrandt, S., and Tromba, A. *The parsimonious universe*. Copernicus, New York, 1996. Shape and form in the natural world.

[17] Hildebrandt, S., and von der Mosel, H. On two-dimensional parametric variational problems. *Calc. Var. Partial Differential Equations 9*, 3 (1999), 249–267.

[18] Hwang, F. K., Richards, D. S., and Winter, P. *The Steiner tree problem*, vol. 53 of *Annals of Discrete Mathematics*. North-Holland Publishing Co., Amsterdam, 1992.

[19] Jarník, V., and Kössler, M. Sur les graphes minima, contenant n points donnés. *Čas. Mat. Fys. 63* (1934), 223–235.

[20] Kröner, H., Novaga, M., and Pozzi, P. Anisotropic curvature flow of immersed networks. *Milan J. Math. 89*, 1 (2021), 147–186.

[21] Mäder-Baumdicker, E. The area preserving curve shortening flow with Neumann free boundary conditions. *Geom. Flows 1*, 1 (2015), 34–79.

[22] Mantegazza, C., Novaga, M., and Tortorelli, V. M. Motion by curvature of planar networks. *Ann. Sc. Norm. Super. Pisa Cl. Sci. (5) 3*, 2 (2004), 235–324.

[23] Montgomery, R. *A tour of subriemannian geometries, their geodesics and applications*, vol. 91 of *Mathematical Surveys and Monographs*. American Mathematical Society, Providence, RI, 2002.

[24] Pan, S., and Sun, J. Curve shortening flow in a 3-dimensional pseudohermitian manifold. *Calc. Var. Partial Differential Equations 60*, 6 (2021), Paper No. 212, 23.

[25] Schmidt, A., and Siebert, K. G. *Design of Adaptive Finite Element Software: The Finite Element Toolbox ALBERTA*, vol. 42 of *Lecture Notes in Computational Science and Engineering*. Springer-Verlag, Berlin, 2005.

[26] Smoczyk, K. Closed Legendre geodesics in Sasaki manifolds. *New York J. Math. 9* (2003), 23–47.